



# **Bachelor Thesis**

in Geoecology

University of Bayreuth

Micrometeorology Group

## **Influence of vegetation density on climate change mitigation potential in a tropical dry forest**



Bayreuth, 21.12.2018

Author: Marie Charlotte Stöckhardt

Supervisor: Prof. Dr. Christoph Thomas

**Details author:**

Marie Stöckhardt (Student Geoecology B.Sc., University of Bayreuth)

Matriculation number: 140 1242

Email: s2mestoe@uni-bayreuth.de

**Auditors:**

Prof. Dr. Christoph Thomas (Micrometeorology Group, University of Bayreuth)

Dr. Wolfgang Babel (Micrometeorology Group, University of Bayreuth)

**Cover picture:**

Tropical dry forest at a firebreak in the dry season in Santa Rosa National Park

Photo taken on 12.05.2018

**Abstract**

The mitigating effect of tropical rain forests on global warming is broadly acknowledged, while the impact of tropical dry forests on climate change is less studied. This thesis investigates climate change mitigation potential (CCMP) of a neotropical dry forest. Five weeks of temperature and humidity measurements at a site in Santa Rosa National Park, Guanacaste, Costa Rica will be presented. CCMP based on the forest's buffering effect on soil and air temperatures was examined and related to vegetation densities. The measuring period includes the transition between the dry and the wet season that are typical for the ecosystem of tropical dry forests. Thus, the data was divided into one week of dry season and four weeks of rainy season. Data was taken daily along four transects of 100m length with a hand carried device with three attached sensors which measured soil temperatures, air temperatures and relative humidity. Additionally, in one transect thermo-hygrometers were installed for automated measurements of air temperatures and relative humidity with a frequency of ten minutes. The CCMP between these transects and within each transect from a clear-cut over the forest edge to the forest interior was compared. The data showed higher temporal than spatial differences with lower temperatures during the rainy season than during the dry season. Spatial differences were higher during the dry season than during the rainy season. The hypothesis of forest transects with denser vegetation having a higher CCMP could partly be verified. During the dry season temperature gradients within the transects from clear-cut to forest interior mostly increased from clear-cut over the area close to the edge into the forest interior. In the rainy season different patterns were obtained for the four transects with the transect in the least dense forest part showing a CCMP decrease from clear-cut to forest interior while the densest forest part showed an increase from clear-cut to the forest. The results highlight, that a protection of tropical dry forests with higher vegetation density which are likely forests in older successional states and a long-term protection of newly afforested tropical dry forests is crucial to contribute to climate change mitigation.



## **Zusammenfassung**

Die mindernde Wirkung von tropischen Regenwäldern auf die globale Erwärmung ist unumstritten, während die Auswirkung von tropischem Trockenwald auf den Klimawandel weniger erforscht ist. Die folgende Arbeit untersucht das Klimaschutzpotenzial eines neotropischen Trockenwaldes im Santa Rosa Nationalpark, Guanacaste, Costa Rica. Anhand von fünfwöchigen Temperatur- und Feuchtemessungen in tropischem Trockenwald wurde das Klimaschutzpotential basierend auf dem Puffereffekt des Waldes gegenüber Boden- und Lufttemperaturen im Hinblick auf Vegetationsdichte untersucht. Der Messzeitraum schließt den Übergang zwischen den zwei für das Ökosystem des tropischen Trockenwaldes typischen Jahreszeiten, Regen- und Trockenzeit ein. Die Daten wurden infolgedessen in eine Woche Trockenzeit und vier Wochen Regenzeit aufgeteilt. Gemessen wurde täglich in vier Transekten mit einer Länge von je 100m mit einem handgetragenen Messgerät an das drei Sensoren zur Messung von Boden-, Lufttemperaturen und relativer Luftfeuchte angeschlossen waren. Zusätzlich wurden Lufttemperaturen und relative Luftfeuchte in einem Transekt zehnmütig von fest installierten Thermohygrometern gemessen. Es wurde zum einen das Klimaschutzpotenzial zwischen diesen Transekten verglichen und zum anderen der Verlauf des Klimaschutzpotenzials entlang der Transekte von der Lichtung über den Waldrand bis ins Waldesinnere. Die zeitlichen Temperaturunterschiede, bei denen die Temperaturen der Regenzeit niedriger waren als die der Trockenzeit, waren höher als die räumlichen Temperaturunterschiede. Diese waren in der Trockenzeit höher als in der Regenzeit. Die Hypothese, dass Transekte an Waldstellen mit dichter Vegetation ein höheres Klimaschutzpotenzial haben, konnte teilweise bestätigt werden. Die Temperaturgradienten innerhalb der Transekte nahmen während der Trockenzeit von der Lichtung zum Waldesinneren hin in den meisten Fällen zu. In der Regenzeit wurden für die vier Transekte verschiedene Ergebnisse ermittelt. Hier lag im Transekt mit der am wenigsten dichten Vegetation eine Abnahme des Klimaschutzpotentials von der Lichtung zum Waldesinneren vor, während dieses im Transekt mit der dichtesten Vegetation vom Waldesinneren zur Lichtung hin abnahm. Diese Ergebnisse zeigen, dass zum einen der Schutz tropischer Trockenwälder mit dichter Vegetation, was meist Wälder in älteren Sukzessionsfolgen sind, und zum anderen die Gewährleistung langfristigen Schutzes wieder bewaldeter tropischer Trockenwälder entscheidend ist, um zum Klimaschutz beizutragen.



**Table of contents**

Abstract .....	iii
Zusammenfassung .....	v
Table of contents .....	vii
List of figures .....	ix
List of tables .....	xiii
List of abbreviations.....	xv
1 Introduction.....	1
1.1 Introduction to tropical dry forests and the study area .....	1
1.2 Study objective and basic concepts.....	1
1.3 Research questions and hypotheses .....	5
2 Materials and methods .....	7
2.1 Field site, measurement devices and setup .....	7
2.2 Overview of data.....	15
2.2.1 Dealing with data gaps.....	15
2.2.2 Delineating functional seasonality.....	19
2.2.3 Comparison of measurement devices .....	22
3 Results.....	29
3.1 Evaluation of vegetation density.....	29
3.2 Comparison of temporal and spatial differences in CCMP.....	32
3.3 Comparison of the four transects regarding CCMP.....	37
3.4 Comparison of gradients of CCMP within the four transects.....	39
4 Conclusion .....	45
Acknowledgements .....	47
Appendix A: Specification measurement devices.....	49
Appendix B: Additional figures .....	51
Appendix C: Additional photos .....	55
Appendix D: Additional tables.....	57

Declaration of Authorship .....	63
5 Publication bibliography .....	59

**List of figures**

figure 1: Temperature distributions of generated example data with and without buffering effect for one day .....	2
figure 2: boxplots of temperature distributions of generated example data with and without buffer effect with the same outliers in both distributions .....	3
figure 3: location of the field site Perros in Santa Rosa National park, Costa Rica .....	7
figure 4: map of the field site showing the location of the four transects and the points of measuring, the location of the weather station and of the stations of the WSN..	8
figure 5: maps of the field site; left: location of the two Northern transects and the Northern measuring location at the clear-cut, the location of the Weather Station and the stations of the WSN; right: location of the Southern transects and the Southern measuring location at the clear-cut.....	9
figure 6: Flow chart of measurement and work process of micrometeorological data..	10
figure 7: Sensors of $M_{man}$ ; a) sensor pt100 for air temperatures; b) thermometer for soil temperatures; c) sensor HWP for air temperatures and relative humidity; d) sensor HWP zoomed in.....	11
figure 8: a) hand-carried thermometer of $M_{man}$ for air temperatures with radiation protection; b) thermo-hygrometer of $M_{aut}$ at the northern clear-cut before radiation protection was attached; c) thermo-hygrometer of $M_{aut}$ at the northern clear-cut with radiation protection; d) weather station; e) WSN1 with radiation protection at the left side.....	13
figure 9: Flow chart of measurements and work process of data on vegetation characteristics.....	14
figure 10: schematic figure of plot for vegetation data around transect .....	14
Figure 11: mean temperatures for each day of the measuring locations in T3 and at the northern clear-cut ( $M_{aut}$ ); legend entries are horizontal distances from transect start .....	15
figure 12: time series of soil temperatures at the measuring locations in each transect with the clear-cuts included in T2 and T4 ( $M_{man}$ ); legend entries are horizontal distances from transect start.....	16

figure 13: time series of air temperatures at the measuring locations in each transect with the clear-cuts included in T2 and T4 ( $M_{\text{man}}$ ); distances in legend entries are horizontal distances from transect start .....	17
figure 14: correlation of temperatures measured by sensor pt100 and sensor HWP ( $M_{\text{man}}$ ) for the four transects without data of 22.05.2018 for T4.....	18
figure 15: mean soil and air temperatures of all measuring locations of the four transects ( $M_{\text{man}}$ ) with cumulative precipitation (weather station) .....	19
figure 16: difference between daily minima and maxima temperatures in T3 ( $M_{\text{aut}}$ ) with cumulative precipitation (weather station).....	20
figure 17: probability density of absolute humidity (left) and air temperatures (right) of all measuring locations in transect 3 in dry and rainy season ( $M_{\text{aut}}$ ).....	21
figure 18: comparison of temperature measurement of $M_{\text{aut}}$ and $M_{\text{man}}$ .....	23
figure 19: mean daily temperatures of the weather station and of $M_{\text{aut}}$ at the 80m measuring location in T3.....	24
figure 20: comparison of absolute humidity of $M_{\text{aut}}$ and $M_{\text{man}}$ .....	25
figure 21: comparison of temperatures of $M_{\text{aut}}$ and WSN 1 .....	26
figure 22: comparison of relative humidity of $M_{\text{aut}}$ and WSN1 .....	27
figure 23: time series of relative humidity of WSN1 .....	27
figure 24: photos of the edge and the forest interior of each transect in the dry season. a) T1 at 15m; b) T2 at 15m; c) T3 at 15m; d) T4 at 15m; e) T1 at 100m, f) T2 at 100m, g) T3 at 100m, h) T4 at 100m .....	31
figure 25: photos of the clear-cut; a) southern measuring location facing north in the dry season; b) southern measuring location facing north in the rainy season; c) northern measuring location facing south in the dry season; d) northern measuring location facing south in the rainy season.....	31
figure 26: photos of the edge and the forest interior of each transect in the rainy season. a) T1 at 15m; b) T2 at 15m; c) T3 at 15m; d) T4 at 15m; e) T1 at 100m, f) T2 at 100m, g) T3 at 100m, h) T4 at 100m .....	32
figure 27: time series of interpolated air temperatures with distance from forest edge in T1 .....	33

figure 28: time series of interpolated soil temperatures with distance from forest edge in T1 .....	33
figure 29: mean air and soil temperatures of all five measuring locations for each transect .....	34
figure 30: probability density of temperatures in T3 for the whole period for all measuring locations; legend entries refer to horizontal distance from transect start .....	35
figure 31: probability density of temperatures in T3 for all measuring locations divided in dry and rainy season .....	35
figure 32: probability density distribution of absolute humidity at all measuring locations in T3 divided in dry and rainy season .....	36
figure 33: mean air temperatures in dry and rainy season of all four transects .....	37
figure 34: mean soil temperatures in dry and rainy season of all four transects.....	38
Figure 35: mean air temperatures divided in clear-cut, edge and forest interior in dry season and rainy season .....	40
figure 36: mean soil temperatures divided in clear-cut, edge and forest interior in dry season and rainy season .....	41
figure 37: Violin plots of air temperatures in the areas clear-cut, edge and forest interior in T3 for dry and rainy season .....	44
figure 38: residuals of comparison of $M_{\text{aut}}$ and $M_{\text{man}}$ in temperatures ( $^{\circ}\text{C}$ ) .....	51
figure 39: residuals of comparison of $M_{\text{aut}}$ and $M_{\text{man}}$ in humidity ( $\text{gm}^{-3}$ ) .....	51
figure 40: time series of interpolated air temperature in T2 .....	52
figure 41: time series of interpolated air temperature in T3 .....	52
figure 42: time series of interpolated air temperature in T4 .....	52
figure 43: time series of interpolated soil temperature in T2.....	53
figure 44: time series of interpolated soil temperature in T3.....	53
figure 45: time series of interpolated soil temperature in T4.....	53



**List of tables**

table 1: location of start and end points of the 4 transects .....	9
table 2: location of the measuring locations at the clear-cut.....	9
table 3: skewness and kurtosis of humidity and temperature distributions separately for dry and rainy season. A negative skewness indicates a left skewed distribution and a positive skewness indicates right skewed distributions. Values for kurtosis below 3 indicate a platykurtic distribution and values above 3 a leptokurtic distribution. .....	21
table 4: functions of calibration of $M_{aut}$ .....	22
table 5: Shapiro Wilk test of normal distribution of residuals of comparison of $M_{aut}$ and $M_{man}$ in temperatures:.....	24
table 6: Shapiro Wilk test of normal distribution of residuals of comparison of $M_{aut}$ and $M_{man}$ in humidity:.....	26
table 7: comparison of vegetation density of the transects in the parameters number of trees/ lianas, mean DBH of trees/lianas, mean tree height, Basal area per hectar of trees/lianas.....	29
table 8: canopy openness in dry and rainy season .....	30
table 9: short-term manual measurements .....	49
table 10: contineous automated measurements.....	49
table 11: weather station .....	50
table 12: Wireless Sensor Network Station 1 .....	50
table 13: photos of the measuring locations at 5m, 30m and 80m from transect start for all transects in the dry season.....	55
table 14: photos of the measuring locations at 5m, 30m and 80m from transect start for all transects in the rainy season.....	55
table 15: mean air and soil temperatures in dry and rainy season of all four transects .	57
table 16: temperature amplitude and interquartile range of temperatures in the different areas in dry and rainy season: .....	57



**List of abbreviations**

CCMP	Climate Change Mitigation Potential
DBH [m]	Diameter at Breast Height
HWP	Hot Wire Probe
IQR	Interquartile Range
M <sub>man</sub>	Manual Measurements
M <sub>aut</sub>	Automated Measurements
T1	Transect 1
T2	Transect 2
T3	Transect 3
T4	Transect 4
WSN	Wireless Sensor Network
WSN1	Station Number 1 of Wireless Sensor Network



## **1 Introduction**

### **1.1 Introduction to tropical dry forests and the study area**

In the current century the multifaceted impacts of global warming show growing evidence. This can be seen in form of e.g. weather extremes getting more abundant, sea water level rise and a reduce of mountain glaciers and icecaps (Diffenbaugh et al. 2017, Raper and Braithwaite 2006). While the importance of tropical rainforests for climate change mitigation is broadly acknowledged, the relation of the ecosystem of tropical dry forests to global warming is less well studied (Sánchez-Azofeifa et al. 2005). Approximately 40% of all tropical ecosystems are covered by tropical dry forests (Cao et al. 2016). The ecosystem's characteristics are a seasonal change between long dry periods and a rainy period with an average annual precipitation of 900 to 2000mm and an average annual temperature of 25°C. Typical vegetation consists of deciduous trees and lianas (Sánchez-Azofeifa et al. 2017). In contrast to tropical rainforests, the land of tropical dry forest is highly suitable for agriculture and livestock. It has therefore undergone a lot of deforestation. (Calvo-Alvarado et al. 2009). Worldwide, approximately 48.5% of tropical and subtropical dry broadleaf forests have already been converted to other land use (Hoekstra et al. 2005). There are only few protected areas of tropical dry forests, as international institutions and local governments concentrated more on other tropical forest types in regards to conservation politics (Sánchez-Azofeifa et al. 2005). The study area analysed in this thesis is one of the protected areas of tropical dry forest. Santa Rosa National Park in Guanacaste, Costa Rica, is part of the National System of Conservation Areas and its dry forest has been recovering from deforestation and has undergone afforestation efforts since the 1980s (Calvo-Alvarado et al. 2009).

### **1.2 Study objective and basic concepts**

The objective of this research is to compare parts of a tropical dry forest in Santa Rosa National Park with differences in vegetation across the dry and the rainy season regarding climate change mitigation potential (CCMP).

Ewers and Banks-Leite (2013) showed that forests have the capability to buffer high and low temperatures and that the microclimate within the forest is consequently different to the one outside. For the temperature distribution over one day, this leads to

a cooling effect inside forests during the day and a warming effect during the night (figure 1). Additionally, maxima and minima temperatures are reached with a time delay in comparison to temperatures without a buffering effect (figure 1). This diurnal cycle applies for most forest types (Li et al. 2015). The strength of this buffering effect will be the basis for the quantification of CCMP in this thesis. Thus, when considering temperatures close to daily maxima, lower temperatures in a forest mean a higher CCMP. Correspondingly, at the time of daily minima, forests with higher temperatures are considered to have a high CCMP. When observing the mean time series of temperatures over the entire diurnal cycle, forest areas which show more constant temperatures have a high buffering effect and therefore a high CCMP.

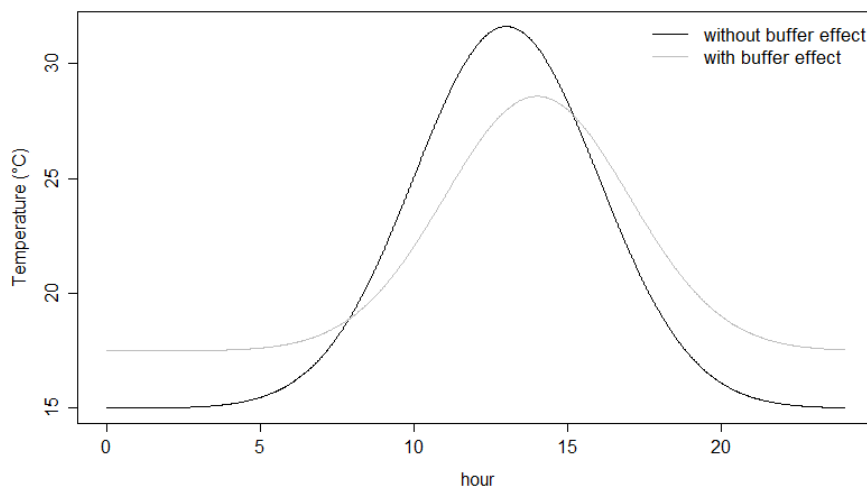


figure 1: Temperature distributions of generated example data with and without buffering effect for one day

The quantification of CCMP won't be based solely on the temperature amplitude, as this is sensible to outliers which can be measurement artefacts. Thus, the whole temperature distributions will be considered with a broader density distribution, meaning a lower CCM, as for these distributions temperature amplitudes are higher and temperature extrema occur more often. Furthermore, the interquartile range (IQR) on which outliers don't have a strong influence will be considered. In figure 2 two outliers were added to the example data of both, the temperature distributions with and without a buffering effect of figure 1. While the amplitude is the same for both data sets now, the boxplots of figure 2 show a higher IQR for the temperatures that weren't influenced by a buffering effect than for the other temperatures. Thus, in case of outliers in the data, the IQR is still a good method to compare the buffering effect between two

different temperature data sets. A low IQR indicates a high buffering effect and hence a high CCMP. A high IQR respectively means a low buffering effect and thus a low CCMP.

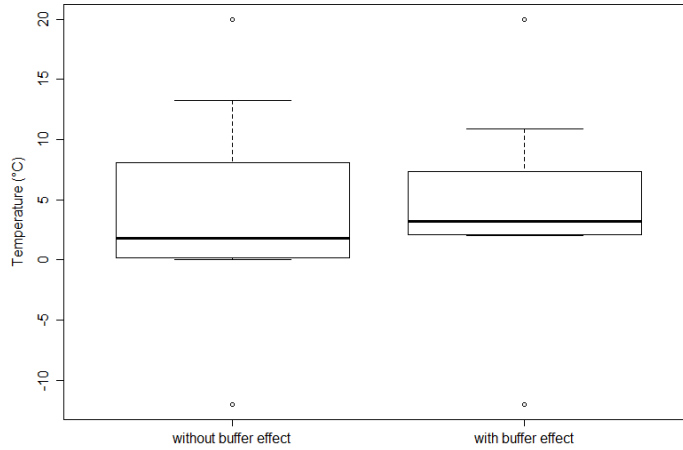


figure 2: boxplots of temperature distributions of generated example data with and without buffer effect with the same outliers in both distributions

Variable CCMP between the compared forest areas can be explained by differences in vegetation which cause different rates of evapotranspiration and albedo. Both influence local patterns of temperatures (Li et al. 2015). The albedo is the fraction of solar radiation that is reflected by the earth's surface (Zvomuya et al. 2008). It can be described as

$$\alpha = - \frac{K \uparrow}{K \downarrow} \quad (1)$$

where  $\alpha$  is the albedo,  $K \downarrow$  is the global solar radiation and  $K \uparrow$  the reflected solar radiation. Both,  $K \downarrow$  and  $K \uparrow$  are thus shortwave radiation components (Foken 2016). Denser forests have a higher amount of green leaves which have a darker colour than grass at clear-cuts or fields, especially when it is dry. Thus, the reflectance of shortwave radiation in denser forest parts is smaller than in sparser forest locations meaning that the albedo is lower. This lower albedo means that more energy is absorbed which leads to a warming effect during the day. The effect of evapotranspiration on temperatures is related to the land surface energy equation (Friedl 2002):

$$-R_n = H + \lambda E + G \quad (2)$$

based on energy conservation, this equation shows that net radiation ( $R_n$ ) equals the product of sensible heat flux ( $H$ ), latent heat flux ( $\lambda E$ ) and soil heat flux ( $G$ ). For

directions towards the surface these terms are defined as positive and for directions away from the surface the signs are negative (Friedl 2002). The net radiation is the available energy at the surface which results from the two shortwave radiative components global solar radiation ( $K \downarrow$ ), reflected solar radiation ( $K \uparrow$ ) and the two longwave radiative components downwelling longwave radiation ( $I \downarrow$ ) and surface radiation ( $I \uparrow$ ) (Foken 2016):

$$R_n = K \downarrow + K \uparrow + I \downarrow + I \uparrow \quad (3)$$

The sensible heat flux is the flux of the energy that leads to a change of the air temperature. The latent heat flux describes the energy which is stored by vaporisation of water and released by condensation of water. Thus, evapotranspiration increases the latent heat flux. Both, sensible and latent heat fluxes are turbulent transport processes. The soil heat flux is the energy transport from or to the surface in the soil and leads to a heating or cooling of the soil. As this process is mainly molecular, it is not very effective. (Foken 2016). A buffering of high temperatures during the day means that the sensible heat flux is reduced while the net radiation stays the same. Equation 2 shows that the sensible heat flux is reduced by an increase of the ground heat flux or the latent heat flux. As the molecular process of the ground heat flux is not very effective, the transformation of energy in form of the latent heat flux is decisive for a loss of latent heat. Thus, an increase of evapotranspiration due to a higher density of plants leads to a decrease of the sensible heat flux. In contrary to the effect of albedo, the effect of evapotranspiration leads to a cooling effect in denser forest parts. Li et al. (2015) examined that in the tropics the cooling effect of evapotranspiration outweighs the warming effect of albedo. Based on this, the effect of evapotranspiration will be considered as decisive in this thesis. Thus, dense forest parts which have higher evapotranspiration rates are expected to have a higher buffering capacity to temperatures and because of that a higher CCMP than sparse forest parts.

The study area is strongly affected by temporal variability of water availability throughout the year, which highly affects the vegetation. At the start of the rainy season water availability is unlimited for plants which induces a growing period of vegetation whereas at the end of the dry season water availability is the lowest of the year. As vegetation characteristics are highly affected by water availability, based on the concept of Thomas et al. (2009) a delineation of seasonality by functionality instead of calendar days will be made in this thesis.

### 1.3 Research questions and hypotheses

To evaluate the following three main research questions, micrometeorological data of air and soil temperatures and data on vegetation density was taken along four different transects from a clear-cut into the forest interior at the study site in Santa Rosa National park Costa Rica.

First, it is of interest whether seasonality or attributes of vegetation impact CCMP stronger to get an estimation on how big the impact of spatial differences in the forest is on CCMP. This is important to estimate whether the goal of conservation efforts aiming for climate change mitigation should be a protection of selected forests with certain vegetation attributes or if a conservation of any area of tropical dry gains a similar effect. Thus, it will be investigated in which of the seasons CCMP is higher and if the temporal differences of CCMP between the two seasons are higher than the spatial differences, leading to the following hypothesis:

- (I) CCMP is higher in the rainy season than in the dry season and spatial differences of CCMP are higher than the temporal ones.

Second, it will be studied if CCMP has a direct connection to vegetation density to estimate whether denser forests which are often forests in a later successional state have a higher CCMP and are thus more important to protect from deforestation in regard of climate change mitigation. The CCMP and vegetation density in the four transects in different locations in the forest will be analyzed and compared to investigate whether locations with higher vegetation densities have a higher CCMP and locations with lower densities have lower CCMP respectively. As rates of evapotranspiration are increased by vegetation, the hypothesis was formulated as:

- (II) CCMP compared between the four transects is higher in transects with high vegetation density than in transects with sparse vegetation.

Third, it is of interest, how the CCMP inside the forest differs to the CCMP at a clear-cut and at the forest near the edge to the clear-cut. For this, the differences of CCMP within each transect will be considered with the aim of evaluating whether fragmentation has a negative impact on the forest's CCMP by increasing the areas that

are close to forest edges. Additionally, the effect of seasonality on the gradients of CCMP within each transect are of interest. The third hypothesis is thus:

- (III) CCMP within a transect increases from clear-cut over the edge into the forest interior and the differences within a transect are higher during the rainy season than during the dry season.

## 2 Materials and methods

### 2.1 Field site, measurement devices and setup

The field site is located in Santa Rosa National Park, Guanacaste, Costa Rica, at an area referred to as Perros (figure 3).

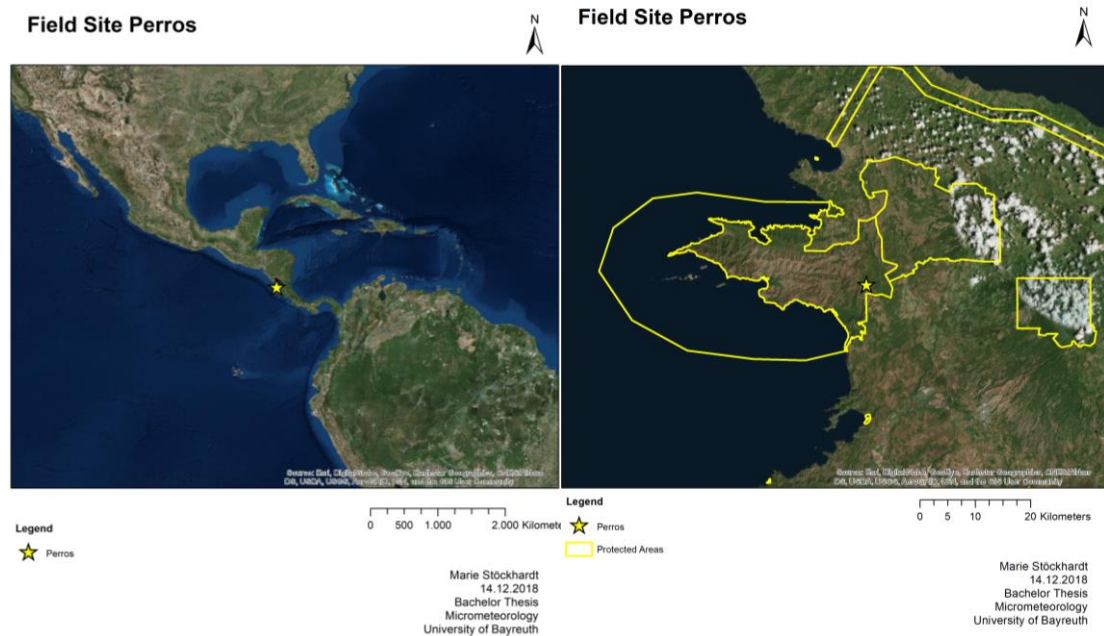


figure 3: location of the field site Perros in Santa Rosa National park, Costa Rica

Measurements were taken in four transects in a tropical dry forest with distinguishable vegetation between the transects on both sides of a 40 to 60 meters broad and more than 2km long fire break (figure 4, table 1). Each transect was perpendicular to the clear-cut and had a length of 100m with 5 measuring locations located at 5m, 15m, 30m, 80m and 100m from the edge of the clear-cut into the forest interior. The length of the transects was chosen equivalent to a study of edge effects on understory microclimate from Portillo-Quintero et al. (op. 2014). An effect of the edge was observed especially for the first 30m from the forest edge into the forest and this effect decreased with further distance from the edge (Portillo-Quintero et al. op. 2014). An investigation by Davies-Colley et al. (2000) of microclimatic edge effects between grazed pasture and a forest showed edge effects of air temperatures reaching a distance of 40m from the open land into the forest interior. Based on these results, the first three measuring locations in the transects at 5m, 15m and 30m from forest edge will be considered as influenced by the edge and will therefore in the analysis be referred to as the edge. The locations in the transects at 80m and 100m from the forest edge will be

called forest interior in this thesis. As shown in figure 2 and 3, two transects were in the North of the clear-cut opposing each other and the other two transects were located approximately 800m further South, also opposite to each other (table 1). The South Eastern transect will be referred to as transect 1 (T1), the South Western as transect 2 (T2). The North Eastern transect will be named transect 3 (T3) and the North Western one transect 4 (T4). Additional measuring will be done at two locations on the fire break in the middle of the two transects North and South respectively (figure 5, table 2).

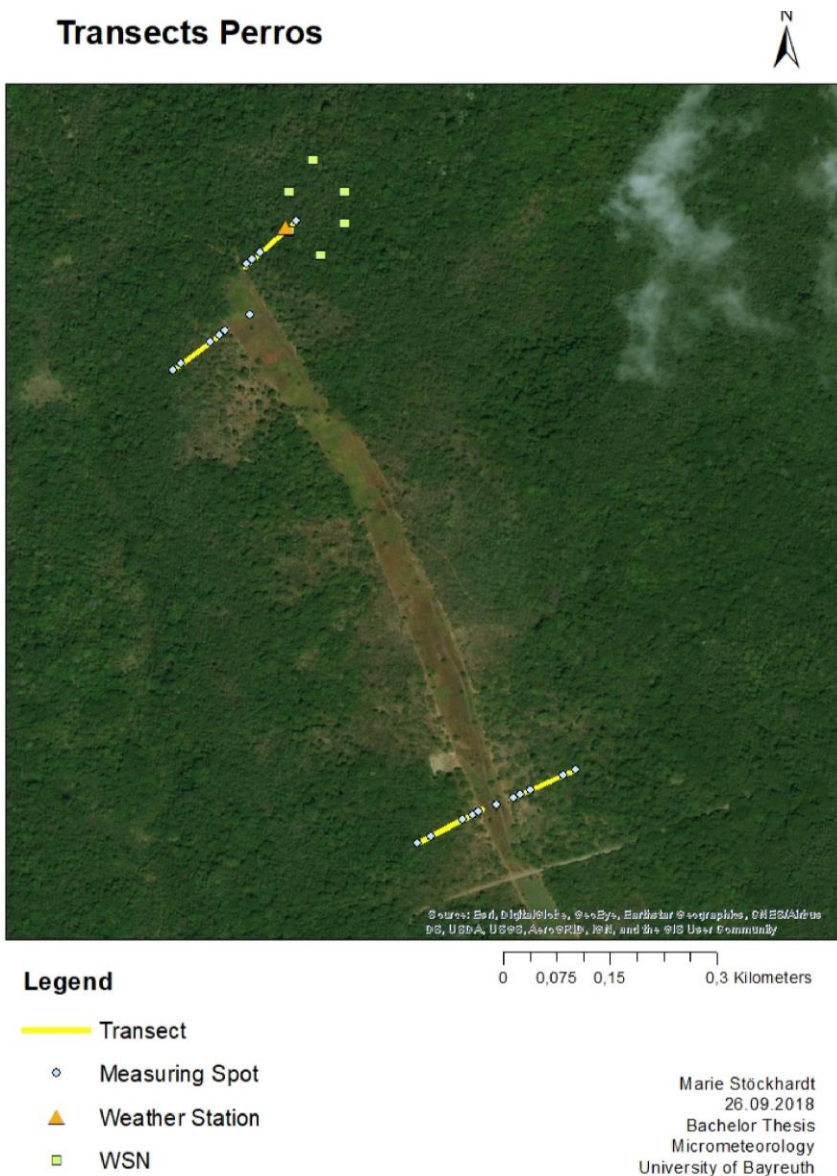


figure 4: map of the field site showing the location of the four transects and the points of measuring, the location of the weather station and of the stations of the WSN

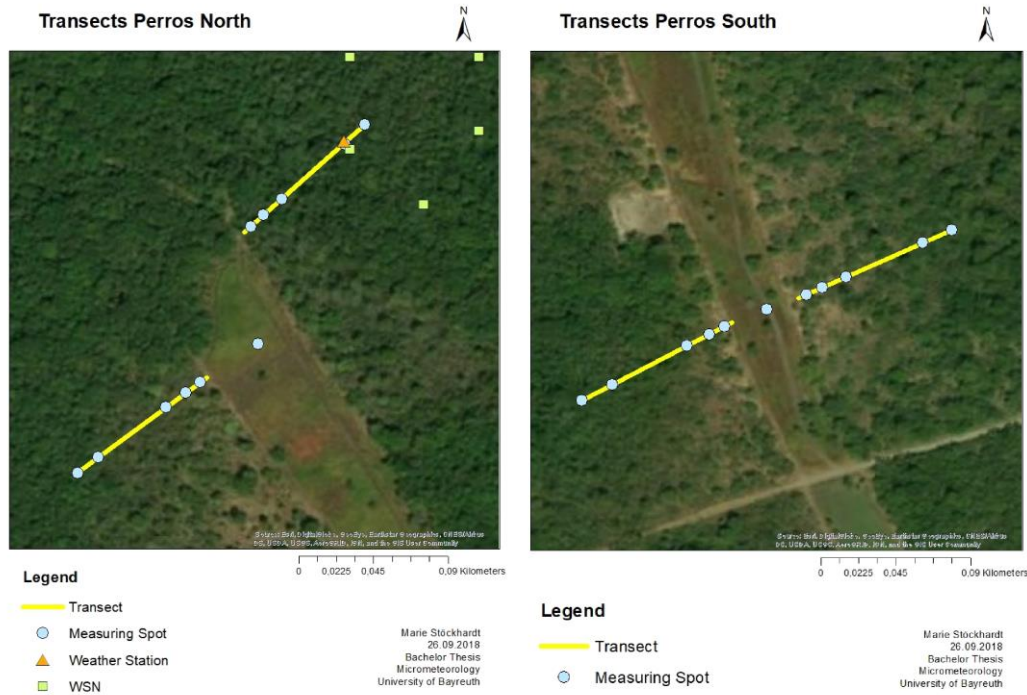


figure 5: maps of the field site; left: location of the two Northern transects and the Northern measuring location at the clear-cut, the location of the Weather Station and the stations of the WSN; right: location of the Southern transects and the Southern measuring location at the clear-cut

table 1: location of start and end points of the 4 transects

		T1	T2	T3	T4
Start point	Latitude	N 10.83632°	N 10.83577°	N 10.843050°	N 10.84226°
	Longitude	W 085.62511°	W 085.62628°	W 085.62847°	W 085.62868°
End point	Latitude	N 10.83669°	N 10.83619°	N 10.84363°	N 10.84174°
	Longitude	W 085,62428°	W 085.62547°	W 085.62782°	W 085.62938°

table 2: location of the measuring locations at the clear-cut

	Clear-cut South	Clear-cut North
Latitude	N 10.83626°	N 10.84244°
Longitude	W 085.62528°	W 085.62840°

Micrometeorological data was measured at the end of the dry season and the start of the rainy season from 09.05.2018 until 13.06.2018 with four different devices. figure 6 gives an overview of the details to the measurements and of the methods applied. All analysis and plots in this thesis were made using the program R, version 1.1.442 (R Core Team 2018).

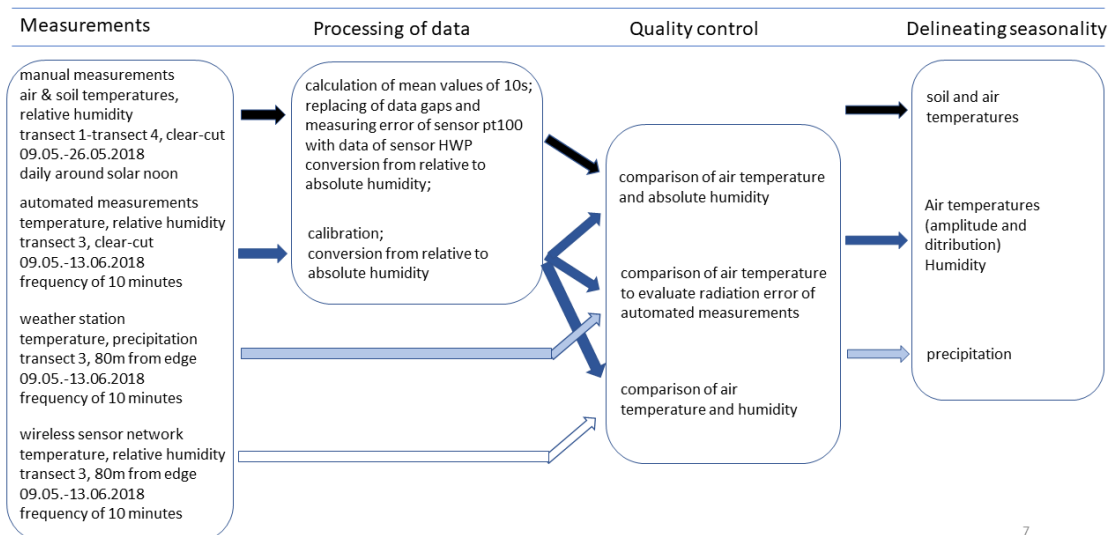


figure 6: Flow chart of measurement and work process of micrometeorological data

In all four transects data were taken at every measuring location with a hand-carried device each day around solar noon from 10:30 LST until 12:30 LST approximately starting at transect 1, going on to 2 and 3 and finishing at transect 4. Three different sensors were attached to the device to measure air temperatures and soil temperatures and relative humidity. The air temperature was measured at a height of 1m and the sensor will be referred to as sensor pt100. A protective radiation shield was made by a plastic cup that was wrapped with aluminium foil and put over the thermometer (figure 8a). The thermometer for soil temperature measured temperatures at the depth of 0.077m from the surface in the soil. Additionally, air temperature and relative humidity were measured at a height of 2m with a hot wire probe. This sensor will be referred to as sensor HWP. Further specifications of the measured parameters and the set-up is given in Appendix A. The data was collected for 10 seconds with a frequency of one second so that 10 values were obtained at every measuring location each day. The data of these 10 seconds was mostly constant, showing that the device was in an equilibrium with the surrounding. In the evaluation the mean value of these 10 seconds will be used. These measurements were performed in the period from 09.05.2018 until 26.05.2018 and will be referred to as manual measurements ( $M_{\text{man}}$ ).

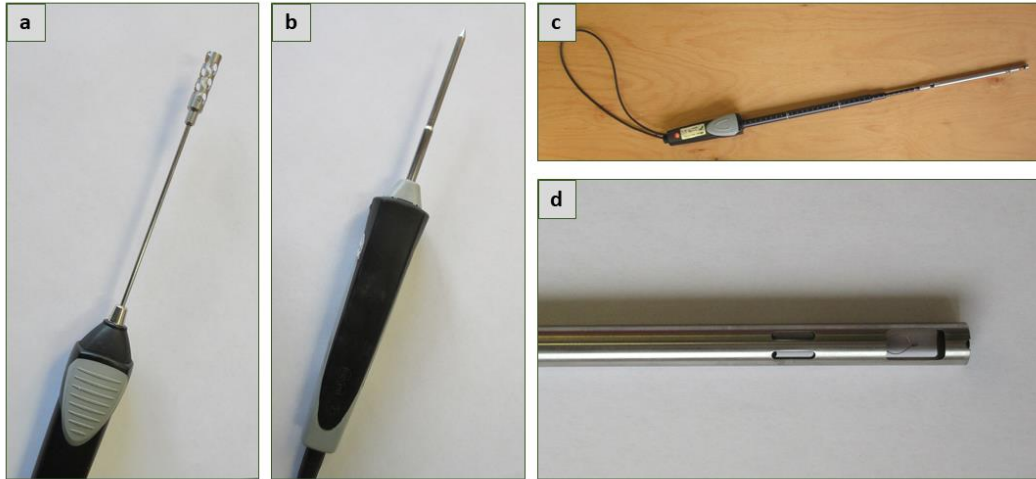


figure 7: Sensors of  $M_{\text{man}}$  ; a) sensor pt100 for air temperatures; b) thermometer for soil temperatures; c) sensor HWP for air temperatures and relative humidity; d) sensor HWP zoomed in

In T3, additionally, six thermo-hygrometers with capacitive semi-conductor sensors were installed at a height of 1m at each measuring location in the transect and at the measuring location on the northern clear-cut for continuous observations (Appendix A). Continuous data of temperature and relative humidity was generated in an interval of 10 minutes from 09.05.2018 until 13.06.2018. To diminish a radiation error of the temperature measurements, double-walled radiation shields with two walls were installed around the thermo-hygrometers (figure 8). These measurements will be referred to as automated measurements ( $M_{\text{aut}}$ ). For an evaluation of the quality control of the micrometeorological data of air temperatures and humidity, the  $M_{\text{aut}}$  will be compared with the  $M_{\text{man}}$  at the measuring locations in T3 and at the northern clear-cut.

For the analysis the measured relative humidity of  $M_{\text{man}}$  and  $M_{\text{aut}}$  was transformed to absolute humidity using the following formulas of relative and absolute humidity and the magnus formula from Foken (2016):

$$\text{Relative Humidity} = \frac{e}{e_s(t)} \cdot 100\% \quad (4)$$

$$\text{Absolute Humidity} = c \cdot \frac{e}{T} \quad (5)$$

$$e_s(t) = c_1 \cdot \exp\left(\frac{c_2 \cdot t}{c_3 + t}\right) \quad (6)$$

with

$e$  = vapour pressure

$e_s(t)$  = saturation vapour pressure

$c = 0.21667 \text{ kg m}^{-3}$

$T$  = temperature in K

$c_1 = 6.112 \text{ hPa}$

$c_2 = 17.62$

$c_3 = 243.12^\circ\text{C}$

$t$  = temperature in  $^\circ\text{C}$ .

Using equation 1 through 3, the following equation can be formed to calculate absolute humidity:

$$\text{Absolute Humidity} = c \cdot \frac{c_1 \cdot \exp\left(\frac{c_2 \cdot t}{c_3 + t}\right)}{T} \cdot \frac{\text{Relative Humidity}}{100\%} \quad (7)$$

At the measuring location at 80m from the forest edge in T3 an automated weather station Ma-4100 was installed at a height of 1m (figure 4, figure 5). Data of air temperatures and precipitation for the entire observational period of the  $M_{\text{aut}}$  from 09.05.2018 until 13.06.2018 was collected (Appendix A). The radiation error is expected to be very small, as the temperature sensor is protected from radiation by the rest of the weather station, while the air ventilation is barely affected (figure 8). The measured air temperatures of  $M_{\text{aut}}$  will be compared with the data of the weather station to estimate the  $M_{\text{aut}}$ 's radiation error.

Besides the above-named measurement devices, there is a station of a Wireless Sensor Network (WSN) located at the 80m measuring location of the north-eastern transect (WSN1), which was installed by the University of Alberta (figure 4, figure 5). This station is installed at a height of 1m and measures different parameters including air temperature and relative humidity in an interval of 10 minutes. A radiation shield is installed to decrease the radiation error (figure 8). The WSN's measuring period is longer than the  $M_{\text{aut}}$ 's. For a further quality control of the collected data, the parameters air temperature and humidity of WSN1 will be compared with the data of  $M_{\text{aut}}$  at the 80m location of T3.

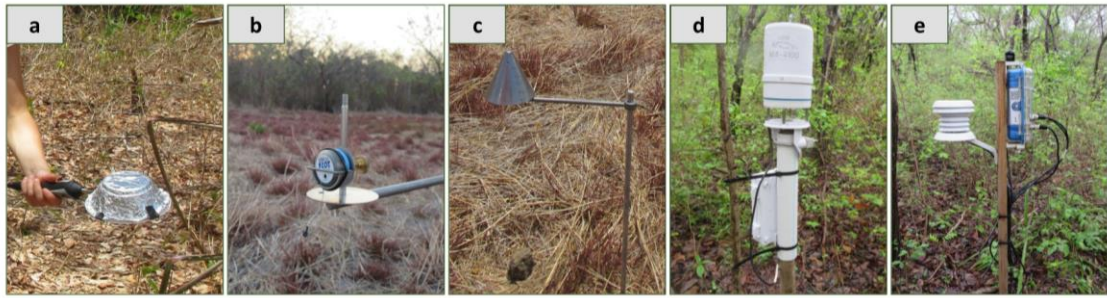


figure 8: a) hand-carried thermometer of  $M_{\text{man}}$  for air temperatures with radiation protection; b) thermohygrometer of  $M_{\text{aut}}$  at the northern clear-cut before radiation protection was attached; c) thermohygrometer of  $M_{\text{aut}}$  at the northern clear-cut with radiation protection; d) weather station; e) WSN1 with radiation protection at the left side

To compare the vegetation characteristics between the forest types in the four transects, several manual measurements were conducted (figure 9). Four plots of 20m times 100m were made going 10m each side from the transects and for the whole length of the transects (figure 10). For each of the plots average diameter at breast height (DBH), basal area per hectare as well as Liana presence or absence was assessed by measuring the trees' and lianas' circumferences for trees with at least 10cm diameter and lianas with at least 5cm diameter. Additionally, average tree height was determined with the help of a laser distance sensor by measuring the distance to the tree and the angle to the highest and the lowest point of the tree. Hemispherical Photos were obtained at every measuring location along the transect once during the dry season and once during the wet season to quantify canopy openness. The calculation of canopy openness was processed with the software Gap Light Analyzer, version 2.0.

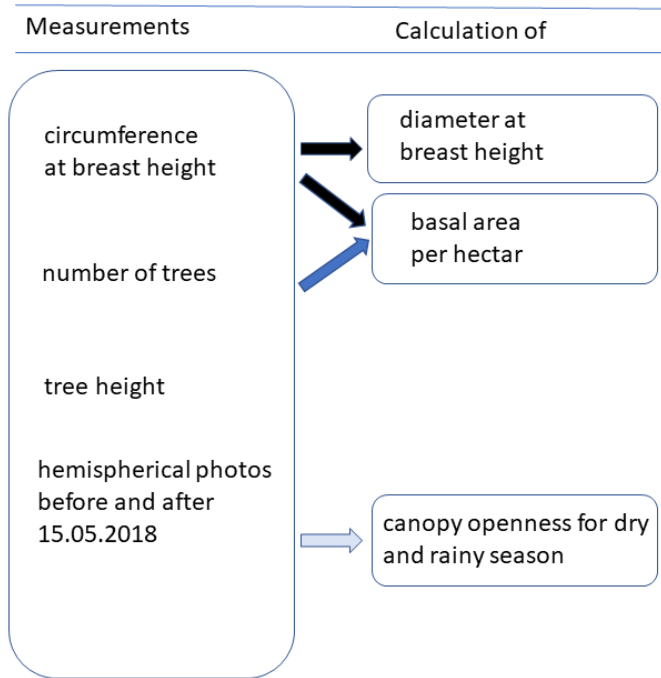


figure 9: Flow chart of measurements and work process of data on vegetation characteristics

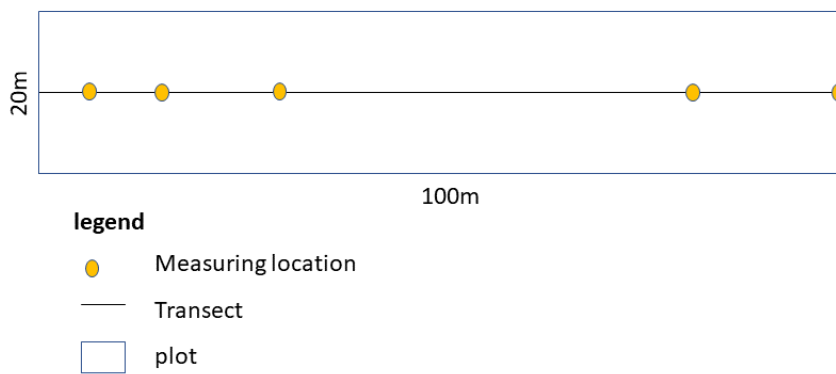


figure 10: schematic figure of plot for vegetation data around transect

## 2.2 Overview of data

### 2.2.1 Dealing with data gaps

The thermo-hygrometers which were stationed at the clear-cut and at the first four measuring locations from the edge into the forest measured without any interruptions from the start until the end of the measuring period (Figure 11). For the location of 100m from transect start, however, there is only data from 24.05.2018 until 13.06.2018, as the data collection for this thermo-hygrometer failed from the start and was exchanged on 24.05.2018. The mean daily temperature on the first day with data at the location of 100m from the forest edge is higher than at the other measuring locations, as the device was exchanged during the day and the data of lower temperatures during the night is missing for 24.05.2018 (Figure 11).

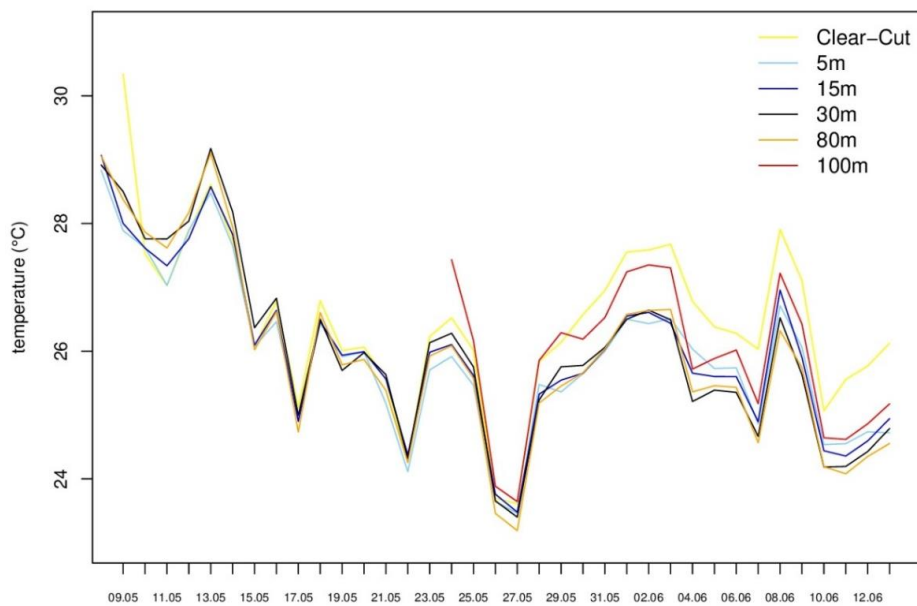


Figure 11: mean temperatures for each day of the measuring locations in T3 and at the northern clear-cut ( $M_{aut}$ ); legend entries are horizontal distances from transect start

The soil and air temperatures collected with the hand-carried device had a few gaps, because the connection of the sensors to the measurement and logging unit sometimes loosened when walking through the forest. When this wasn't noticed, and the sensors weren't reattached properly, no data was collected. As shown in the time series in figure 12, for the soil temperatures this happened three times: in T2 at 100m from transect start on 13.05.2018, in T3 at 80m on 09.05.2018 and in T4 at 30m on 26.05.2018.

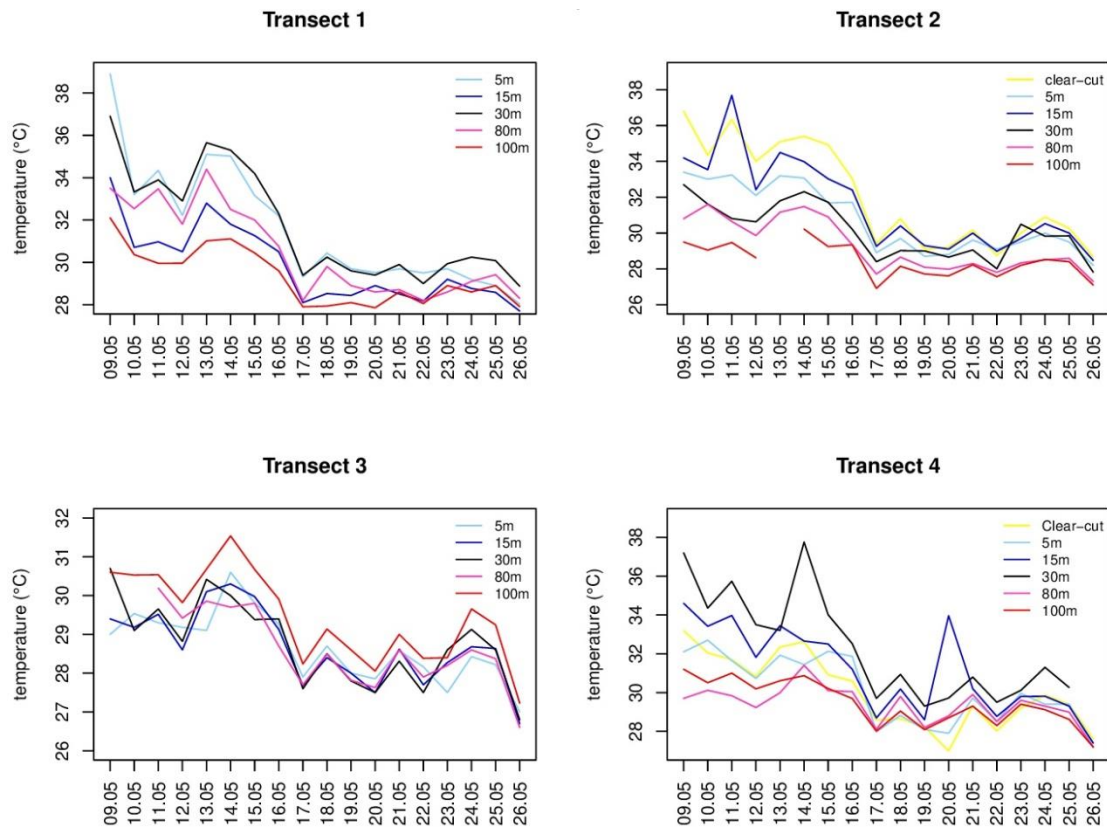


figure 12: time series of soil temperatures at the measuring locations in each transect with the clear-cuts included in T2 and T4 ( $M_{\text{man}}$ ); legend entries are horizontal distances from transect start

In the time series of the air temperatures in figure 13 it can be seen, that there are some data gaps, too: In T1 the data of 23.05.2018 is missing for the locations at 30m, 80m and 100m and in T2 the data of the same date is missing for all measuring locations. For T3 and T4 all data was collected, however on 22.05.2018 in T4 the measured air temperatures ranged from 14°C to 22°C at the 5 measuring locations. As this is more than 10K below the range of temperatures measured in the rest of the period in all four transects, it is assumed that a measuring error occurred.

A clear decrease of temperatures in the last two days for all transects for soil and air temperatures was observed (figure 12, figure 13). This can be explained by nontypical weather conditions of constant gentle rainfall during most of the day and night in the end of the measuring period. On the other days in the wet season in the measuring period, rain typically fell only in the afternoon, with higher rates, while there was no precipitation during the rest of the day and night.

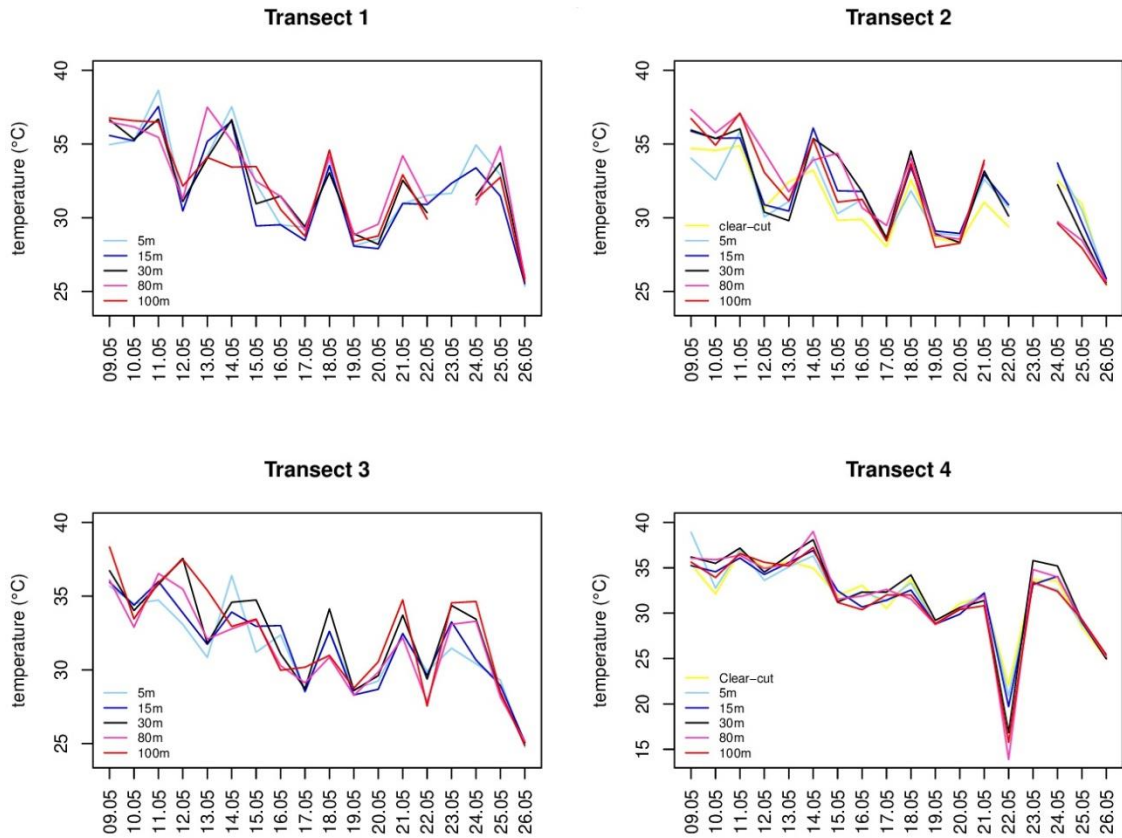


figure 13: time series of air temperatures at the measuring locations in each transect with the clear-cuts included in T2 and T4 ( $M_{\text{man}}$ ); distances in legend entries are horizontal distances from transect start

As air temperatures were measured with two different sensors (sensor pt100 and sensor HWP) on the two different heights of 1 meter and 2 meters at the same locations and at the same times, a comparison between those two measurements can be made (figure 14). For T4 the data of 22.05.2018 was excluded because it contains outliers in the data of sensor pt100 due to the measuring error on that day. The scatter plots of the data showed, that the sensors measured similar temperatures for the four transects, with a good fit of a linear model with  $R^2$  values above 0.9. The fit lines have slopes differing from unity not more than 0.11 and offsets below  $0^\circ\text{C}$ , showing that the linear fit is similar to the line of  $x$  equaling  $y$  (figure 14). Due to the good agreement between data from the two sensors despite differences in measurement height, missing data as well as the measurement error in T4 of sensor pt100 will be replaced by the data of sensor HWP.

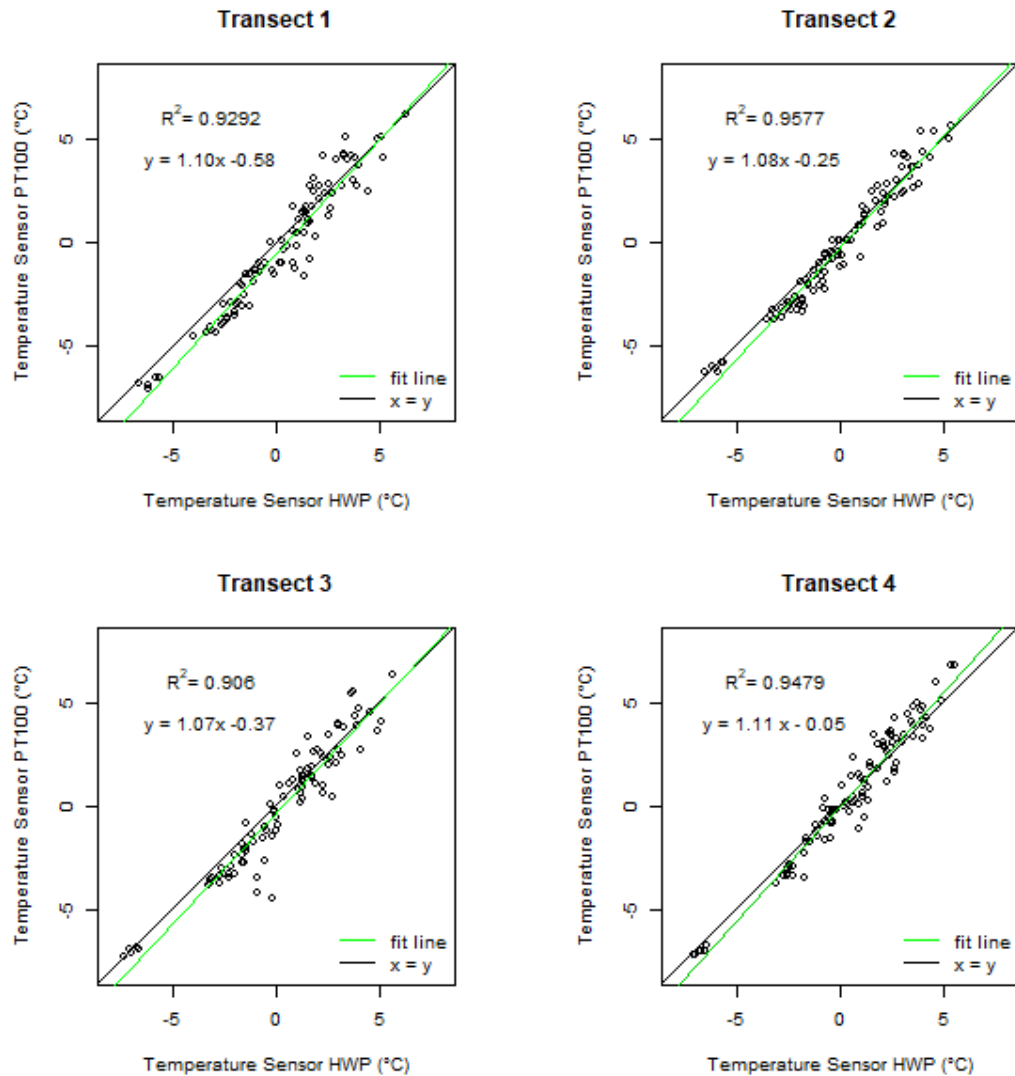


figure 14: correlation of temperatures measured by sensor pt100 and sensor HWP ( $M_{\text{man}}$ ) for the four transects without data of 22.05.2018 for T4

An interpolation of the data of  $M_{\text{man}}$  for the distances within the transects for the whole measuring period was made using the method akima. This interpolation method is based on a piecewise function build of a set of polynomials of third degree (Akima 1974).

### 2.2.2 Delineating functional seasonality

The ecosystem tropical dry forest, in which the measurements are performed, is highly affected by its two functional seasons. The dry season extends from December until May (Sánchez-Azofeifa et al. 2017). The measuring period from 09.05.2018 until 13.05.2018 is therefore at the transition of the dry season to the wet season and the data will be divided into these two functional seasons. The decision on which day the rainy season started, will be made on the base of the precipitation rates during the measuring period. When looking at the cumulative precipitation for the measuring period in figure 15 and figure 16, one can see that there was nearly no rain until 15.05.2018. Therefore, the time before 15.05.2018 is considered as the dry season and the data that was taken on 15.05.2018 and later will be referred to as belonging to the rainy season. The change of seasons can also be seen when looking at the temperatures: soil and air temperatures were lower in the time after 15.05.2018 than before and the daily temperature amplitude is in general higher before the change of the seasons than afterwards (figure 15, figure 16).

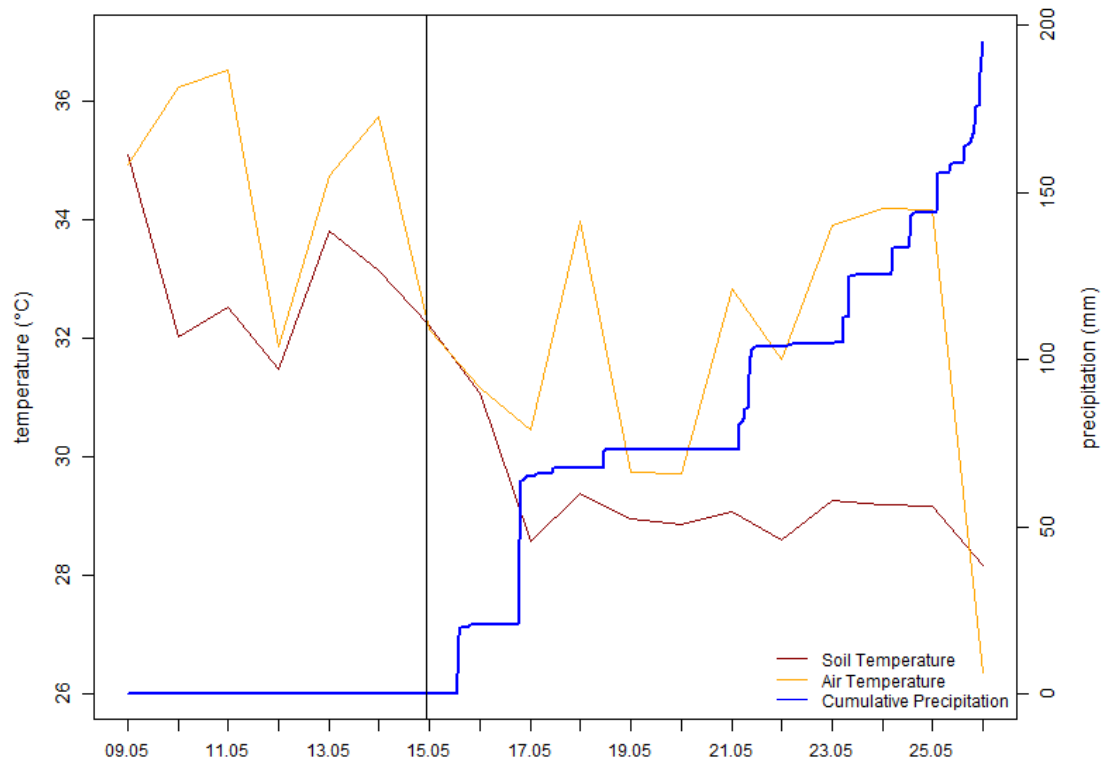


figure 15: mean soil and air temperatures of all measuring locations of the four transects ( $M_{\text{man}}$ ) with cumulative precipitation (weather station)

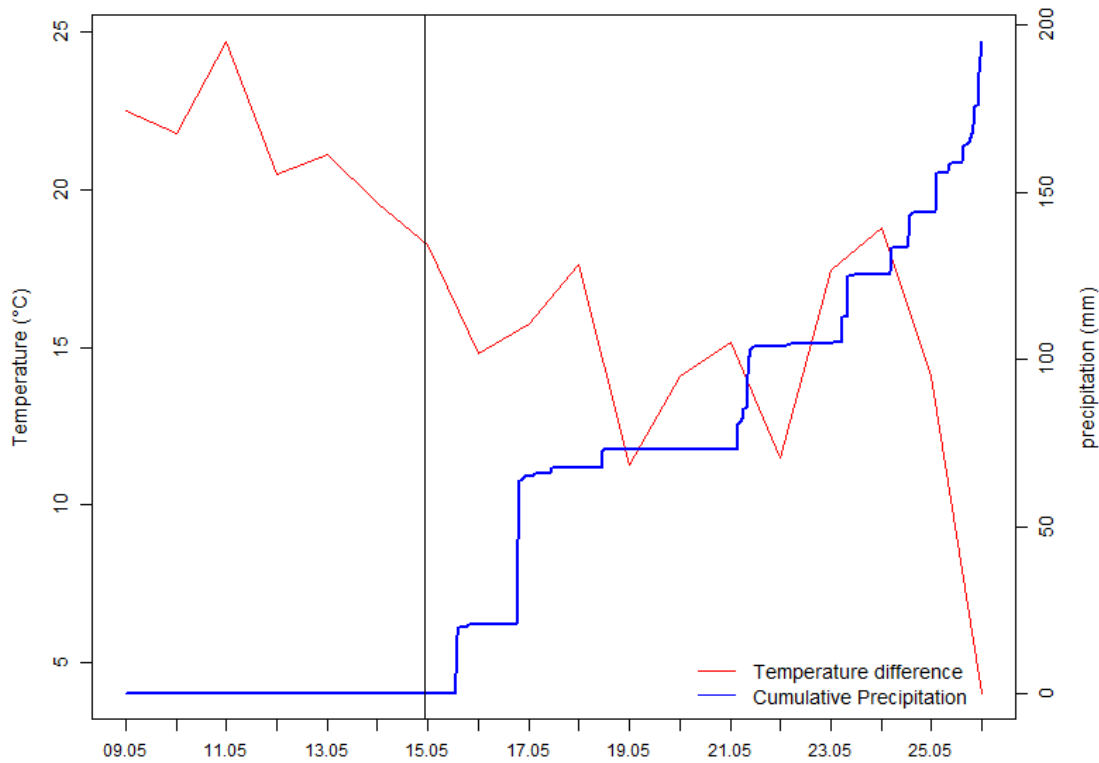


figure 16: difference between daily minima and maxima temperatures in T3 ( $M_{\text{aut}}$ ) with cumulative precipitation (weather station)

Absolute humidity measured by  $M_{\text{aut}}$  in transect 3 separately for the time before and after 15.05.2018 also supports the division into two seasons. A clear difference in the probability density distributions of dry and rainy season can be seen, as the distribution of the probability density of the humidity shifts to higher values in the rainy season than in the dry season for the minima as well as the maxima (figure 17). The values of skewness and kurtosis of the humidity distribution indicate right skewed and leptokurtic distributions, as the values for skewness are positive and the values of the kurtosis are above three for both seasons. Both, skewness and kurtosis are increasing from rainy to dry season (table 3). Furthermore, in contrast to the dry season, in the rainy season there is a second smaller peak at higher values than the main one which represents the data that was taken while it was raining (figure 17). The probability density plot of temperatures divided in both seasons shows a shift of the whole distribution but does also show increased values for skewness and kurtosis from dry to rainy season (figure 17, table 3). The distributions for both seasons are left-skewed, but in the dry season it is platykurtic while in the rainy season it is leptokurtic, meaning that the temperatures are more spread out in the dry season with higher probabilities for low and for high temperatures (figure 17, table 3). Additionally, for the dry season there is a second peak for temperatures between 32 to 35 °C. A similar peak during the

rainy season is lesser pronounced and at cooler temperatures (figure 17). These clear differences between the two density distributions support the division of the data into two functional seasons before and after 15.05.2018.

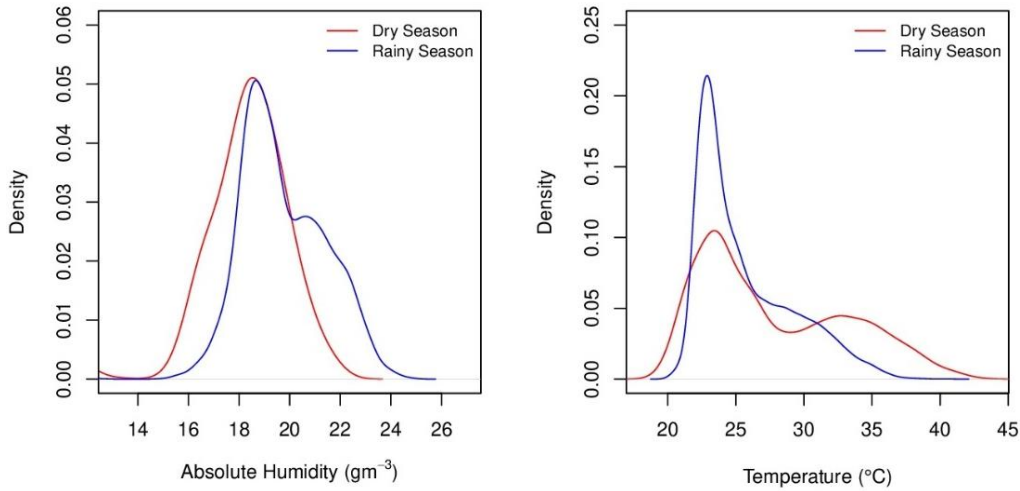


figure 17: probability density of absolute humidity (left) and air temperatures (right) of all measuring locations in transect 3 in dry and rainy season ( $M_{aut}$ )

table 3: skewness and kurtosis of humidity and temperature distributions separately for dry and rainy season. A negative skewness indicates a left skewed distribution and a positive skewness indicates right skewed distributions. Values for kurtosis below 3 indicate a platykurtic distribution and values above 3 a leptokurtic distribution.

	skewness dry season	skewness rainy season	kurtosis dry season	kurtosis rainy season
Distribution of humidity	1.3	1.6	3.2	3.8
Distribution of temperatures	0.6	1.0	2.2	3.1

### 2.2.3 Comparison of measurement devices

To maximize measurement accuracy of the thermo-hygrometers, calibration measurements for temperature and humidity for the six devices were performed. For both, the temperature and humidity calibration one measurement was performed in an insulated chamber at room temperature (26°C) and a relative humidity of 49%. A pt100 temperature sensor was placed into the insulated chamber for reference. For humidity the mean values of the thermo-hygrometers were used as a reference. A second measurement for the temperature calibration was done in a refrigerator at 12°C. Here the mean temperature of the six thermo-hygrometers was used as the reference temperature. For the humidity calibration a second measurement was done in a box with an increased relative humidity of 94% using a ventilator to ensure constant conditions in the whole box. Again, the mean humidity values of the six thermo-hygrometers was taken as reference. Based on these measurements, calibration lines for the devices of  $M_{\text{aut}}$  were calculated (table 4). All positive offsets are mathematically compensated by slopes below 1 and all negative offsets by slopes above 1. Thus, by calculating the modified values using the functions of the calibration lines, the change of the data was small despite sensor-specific large deviations of over 1°C for temperature and of 4.5% and 5% for relative humidity (table 4).

table 4: functions of calibration of  $M_{\text{aut}}$

Measuring location of device	Function of calibration line temperature (x = temperature in °C)	Function of calibration line relative humidity (x = relative humidity in %)
Clear-Cut	$1.02 x - 0.59^{\circ}\text{C}$	$0.98 x + 0.97\%$
5m	$0.95 x + 1.31^{\circ}\text{C}$	$0.91 x + 5.00\%$
15m	$0.99 x + 0.55^{\circ}\text{C}$	$1.02 x - 0.99\%$
30m	$1.03 x - 0.27^{\circ}\text{C}$	$0.97 x + 2.28\%$
80m	$1.04 x - 1.26^{\circ}\text{C}$	$1.10 x - 4.50\%$
100m	$1.03 x - 0.64^{\circ}\text{C}$	$1.05 x - 3.51\%$

A comparison of the thermo-hygrometers' data with the hand-carried device's data was made to evaluate its accuracy. To this end, the data of temperature and humidity from T3 was compared for each measurement location, taking the measuring time of the  $M_{\text{aut}}$  which was closest to the time at which the  $M_{\text{aut}}$  was taken for each day. For the comparison the data of both devices was standardized. For this the mean temperature

value of both datasets was calculated and subtracted from every datapoint. At the first three measuring locations of T3 a linear model shows good fits with  $R^2$  values of approximately 0.9. With 0.8 and 0.7 they are a bit smaller for the 80m and 100m location. The offsets are positive for all measuring locations varying from  $0^\circ\text{C}$  to  $3^\circ\text{C}$  and the slopes are mostly about 1 (figure 18). The positive off-sets in addition to slopes of 1 show that the data of  $M_{\text{aut}}$ , which is displayed on the y-axis of figure 18, exceed those of the data of  $M_{\text{man}}$ .

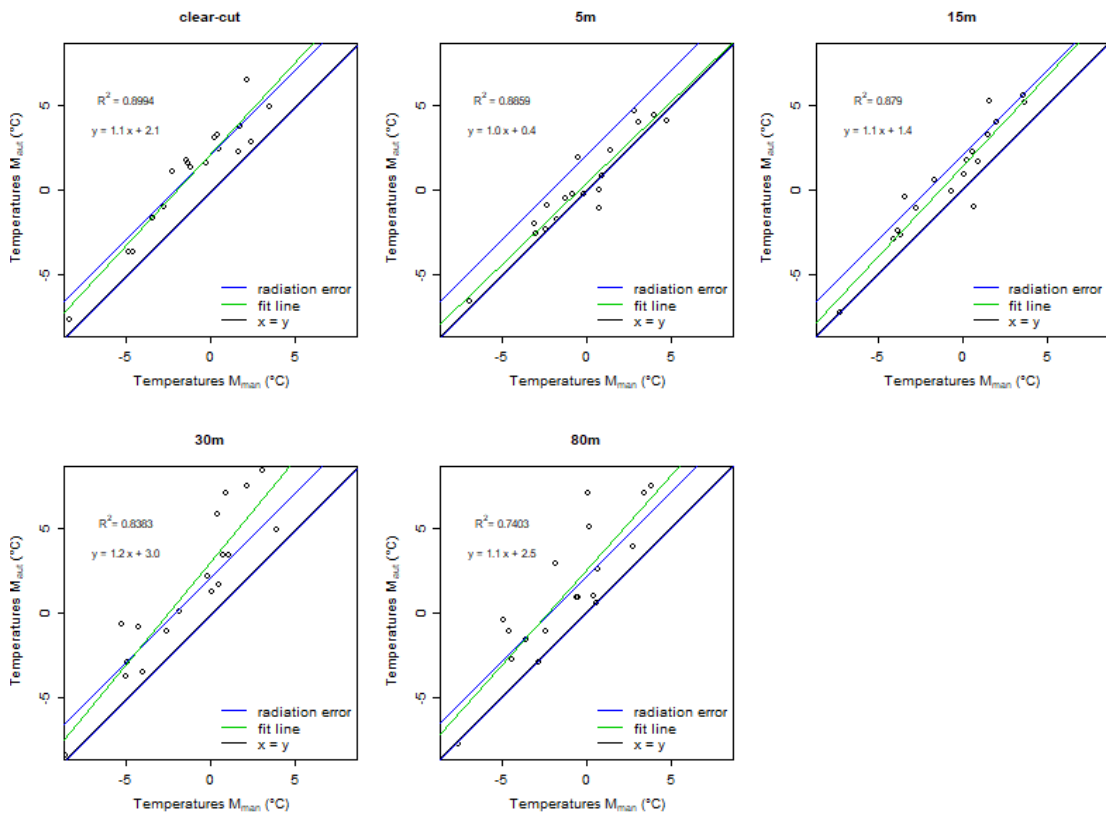


figure 18: comparison of temperature measurement of  $M_{\text{aut}}$  and  $M_{\text{man}}$

Differences can partly be explained by a radiation error of  $M_{\text{aut}}$  which, at the time of the measurements close to solar noon, led to a measurement of higher temperatures than the actual ones. The reason of the higher radiation error of  $M_{\text{aut}}$  in comparison to  $M_{\text{man}}$  probably is a lower ventilation of the thermo-hygrometers. The installed radiation protection surrounds the  $M_{\text{aut}}$  and thus reduces the movement of the air at the device. The  $M_{\text{man}}$ 's radiation protection on the other hand was more open and additionally the sensor was hand-carried and thus moved. With that a better ventilation could be ensured. The  $M_{\text{aut}}$ 's radiation error was quantified by comparing the mean daily temperatures of  $M_{\text{aut}}$  with the data of the weather station at 80m in T3. The radiation error of the weather station was low, as a protection was given without affecting the

ventilation. Hence, the differences of 0.1K between temperature minima and 2.1K between temperature maxima in this comparison are considered to be the result of the radiation error of  $M_{\text{aut}}$  (figure 19). Thus, differences in observations of  $M_{\text{aut}}$  and the  $M_{\text{man}}$  which lie within this range can be due to the radiation error.

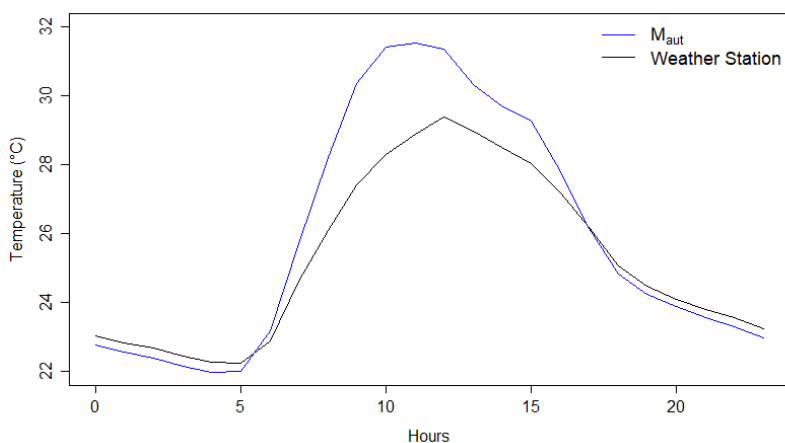


figure 19: mean daily temperatures of the weather station and of  $M_{\text{aut}}$  at the 80m measuring location in T3

Reasons for varying data between the two different devices outside of this range could be due to the  $M_{\text{man}}$  being hand-carried and the exact locations and time of  $M_{\text{man}}$  differing from day to day and not being exactly the same as for  $M_{\text{aut}}$ . The turbulent exchange of air and heat fluxes may have varied on a small scale in space and time and have led to differences between the two measurements. A systematic error in the data of the comparison can be excluded by looking at the distribution of the residuals (figure 38). A Shapiro Wilk test of normal distribution which tests the closeness of the data yields p-values above 0.05 which means that the residuals follow a normal distribution (table 5).

table 5: Shapiro Wilk test of normal distribution of residuals of comparison of  $M_{\text{aut}}$  and  $M_{\text{man}}$  in temperatures:

Measuring location	P-value	Normal distribution
Clear-cut	0.97	Yes
5m	0.93	Yes
15m	0.06	Yes
30m	0.14	Yes
80m	0.25	Yes

To compare the data of absolute humidity between  $M_{aut}$  and  $M_{man}$ , the data of absolute humidity was standardized by subtracting the mean value of absolute humidity of both datasets from every datapoint. Differences between the automated and the manual measurements are higher for absolute humidity than for temperatures. The  $R^2$  values for the linear model fit for the correlation range from an  $R^2$  value of 0.5 to 0.8 and the linear models have slopes between 0.6 and 0.8 with off-sets between -0.9 and 2.1  $gm^{-3}$ . The mostly positive off-sets in combination with slopes below 1 mean that neither of the two devices generally measured higher or lower values of humidity than the other (figure 20).

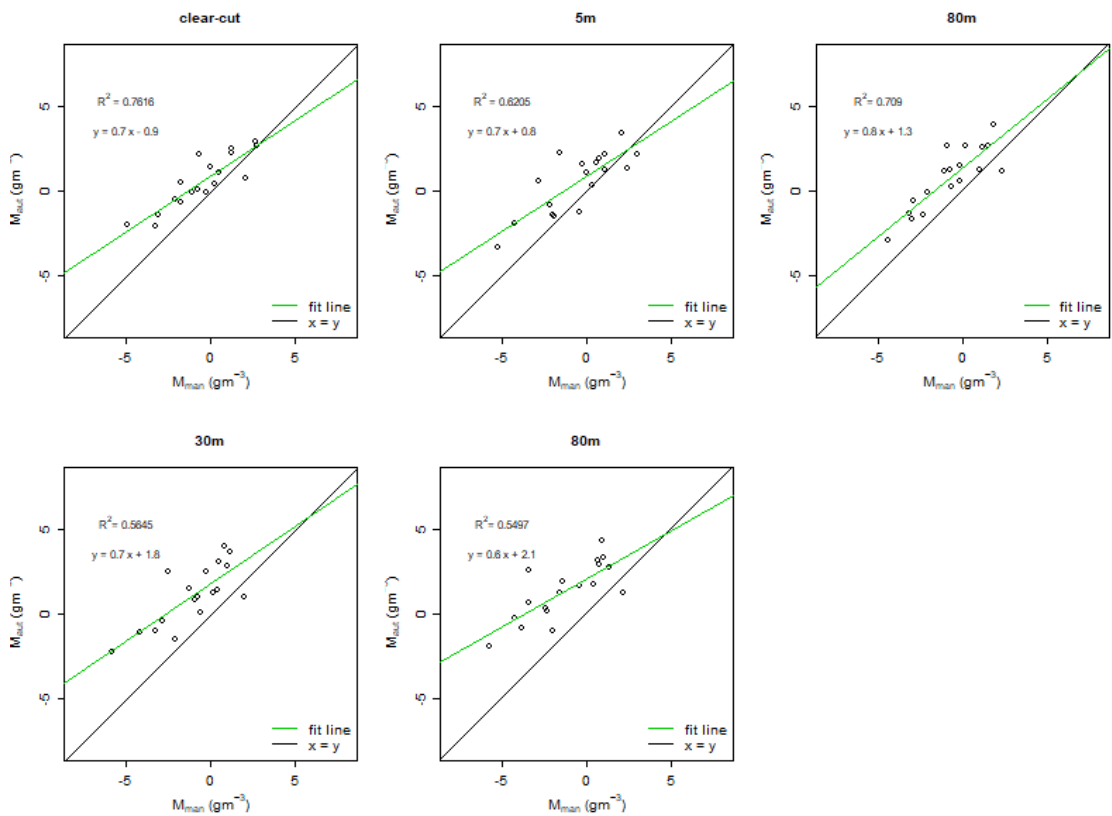


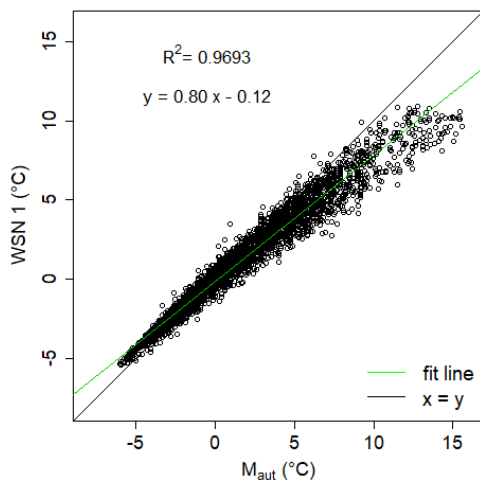
figure 20: comparison of absolute humidity of  $M_{aut}$  and  $M_{man}$

The deviation between the two measurements is likely due to the different age of both devices. As the device of  $M_{man}$  was new before this research was started, a higher quality of its data is expected in comparison to the devices of the  $M_{aut}$  where a degradation of the humidity measurement with the time is expected. An analysis of the residuals, shows that the residuals have p-values of above 0.05 for the Shapiro Wilk test and thus follow a normal distribution, indicating that there is no further systematic mistake (figure 39, table 6).

table 6: Shapiro Wilk test of normal distribution of residuals of comparison of  $M_{\text{aut}}$  and  $M_{\text{man}}$  in humidity:

Measuring location	P-value	Normal distribution
Clear-cut	0.98	Yes
5m	0.86	Yes
15m	0.86	Yes
30m	0.97	Yes
80m	0.54	Yes

In addition to the comparison of  $M_{\text{aut}}$  and  $M_{\text{man}}$  the data of  $M_{\text{aut}}$  was compared with the data measured by WSN1. There was a good fit of a linear model with  $R^2$  being nearly 1 (figure 21). The slope is with 0.8 below 1 and the fit line has a negative offset of  $-0.12^\circ\text{C}$  (figure 21). As the station of the WSN is displayed on the y-axes, the  $M_{\text{aut}}$  had slightly higher values than the WSN1. The deviation from the WSN's data increased with higher temperatures. This is likely due to a higher radiation error of  $M_{\text{aut}}$  in comparison to WSN1 (figure 21).

figure 21: comparison of temperatures of  $M_{\text{aut}}$  and WSN 1

For the comparison of the measurements of relative humidity of the two devices the data was also standardized by subtracting both dataset's mean value from every datapoint. The linear correlation was very low with an  $R^2$  value of less than 0.1. The slope of the fit line was nearly 0 and there was a high off-set of 97 % (figure 22).

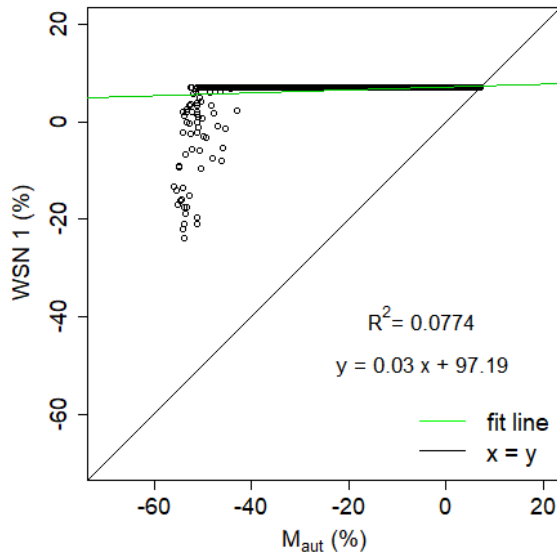


figure 22: comparison of relative humidity of  $M_{aut}$  and WSN1

The low correlation can be explained by a measuring error in the humidity measurements that occurred for the WSN1 for the whole measuring period of the  $M_{aut}$ . The data shows values of 100% relative humidity during most of the days in this period and just a few other values which are between 70% and 100% (figure 23). Physically this data is very unlikely as this would mean a nearly constant saturation. Especially in the dry season in a tropical dry forest where there is a low water availability, these values can be excluded.

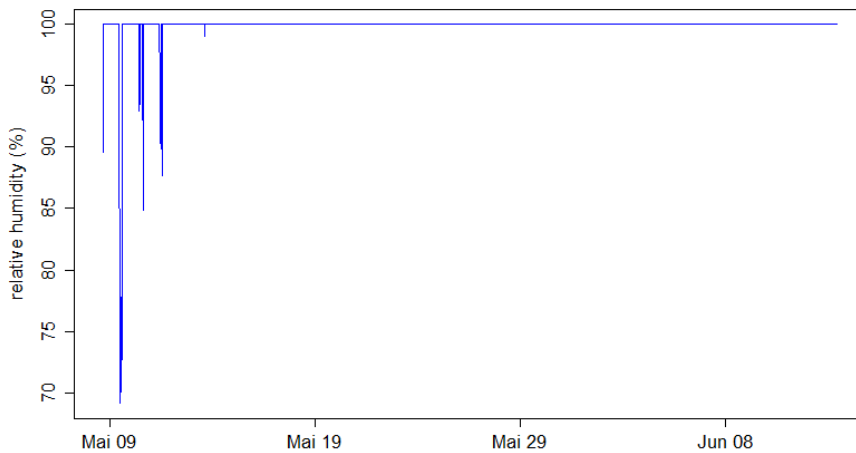


figure 23: time series of relative humidity of WSN1



### 3 Results

#### 3.1 Evaluation of vegetation density

The analysis of vegetation density for the plots around each transect showed that T2 and T4 in comparison to the other two plots had more trees with a number of 78 and 89, but a lower DBH of 0.15 m (table 7). In the plot around T1 there were 24 trees, which is by far the lowest amount for the four plots while the plot around T3 had only one tree less than T2. Both, the plots of T1 and T3 had a mean DBH of 0.17m (table 7). The basal area per hectare had the lowest result for the plot around T1 with 5.0 m<sup>2</sup> ha<sup>-1</sup> and the highest result for the plot around T3 which is 13.0 m<sup>2</sup> ha<sup>-1</sup>. The plots of T2 and T4 were quite close to each other with 9.1 m<sup>2</sup> ha<sup>-1</sup> and 9.8 m<sup>2</sup> ha<sup>-1</sup> (table 7). This put the four plots in the order of T1 being in the least dense plot followed by T2 and T4 while T3 had the highest density of vegetation. The comparison of the openness of the canopies in the four transects showed the same order of the four transects with a high canopy openness meaning a low canopy density. T1 had the highest canopy openness with an average of the 5 measuring locations of 66% in the dry season and 56% in the rainy season (table 8). T2 and T4 resembled each other, but T4 had a lower canopy openness. T3 had the lowest canopy openness and with that the highest canopy density (table 8). The measured tree heights also put the transects in the same order with T1 having the lowest trees with an average of 5m, T3 having the highest trees with an average of 11 meters and T2 and T4 being in between with 8m and 9m respectively (table 7). Lianas were absent for T3 while there was one in T1, two in T4 and three in T2. As the mean DBH of lianas was 0.06m for all three transects with lianas, T2 with the most lianas had the highest basal area followed by T2 (table 7).

table 7: comparison of vegetation density of the transects in the parameters number of trees/ lianas, mean DBH of trees/lianas, mean tree height, Basal area per hectar of trees/lianas

	Plot 1	Plot 2	Plot 3	Plot 4
Number of Trees	24	78	77	89
Mean DBH (m)	0.17	0.15	0.17	0.15
Mean Tree Height (m)	5	8	11	9
Basal area per hectar (m <sup>2</sup> ha <sup>-1</sup> )	5.0	9.1	13.0	9.8
Number of Lianas	1	3	0	2
Mean DBH Liana (m)	0.06	0.06	-	0.06
Basal area per hectar liana (m <sup>2</sup> ha <sup>-1</sup> )	0.01	0.03	-	0.04

table 8: canopy openness in dry and rainy season

	Dry season				Rainy season			
	T1	T2	T3	T4	T1	T2	T3	T4
5m	79 %	61 %	35 %	56 %	60 %	45 %	32 %	31 %
15m	63 %	62 %	36 %	60 %	48 %	46 %	23 %	26 %
30m	73 %	56 %	30 %	64 %	68 %	33 %	19 %	30 %
80m	67 %	54 %	32 %	44 %	62 %	27 %	21 %	21 %
100m	49 %	48 %	39 %	43 %	42 %	27 %	26 %	24 %
average	66 %	56 %	34 %	53 %	56 %	36 %	24 %	26 %

The differences between the vegetation density at each of the five measuring locations in the transects were evaluated visually and by analysing canopy openness. For T1 the measuring locations in the edge at 5m and 30m were very open while the location at 15m had more vegetation, but still a high canopy openness (figure 24, table 8). The forest interior's vegetation was denser with a low canopy openness at the 100m measuring location compared to the rest of the transect. During the dry season there was nearly no green vegetation in the whole transect 1 (figure 24, table 13). T2 had denser vegetation at the edge than T1, which became even denser when going to the forest interior. This was reflected in the canopy openness where the openness decreased from 5m to 100m except for a slight increase from 5m to 15m (table 8). Along the whole transect there was vegetation with green leaves during both seasons (figure 24, figure 26). In T3 the edge's vegetation density was higher than in the other transects with generally increasing density from 5m to 30m. The density was decreasing from 30m to 80m where the canopy openness was lower than at the 5m and 15m location. To the 100m location it decreased further, so that this location had the highest canopy openness in T3 during the dry season and the second highest during the wet season (table 13, table 8). The lowest values of canopy openness were calculated for the 30m measuring location (table 8). The third transect had distinguishably more green vegetation than the other transects during both seasons (table 13, table 14). In T4 the canopy openness showed lower values for the measuring locations at 80m and 100m than at the edge which means that the vegetation was denser for the forest interior than for the forest edge (table 8). The edge had almost no green vegetation during the dry season, while the forest interior had green leaves for both seasons (figure 24, figure 26).

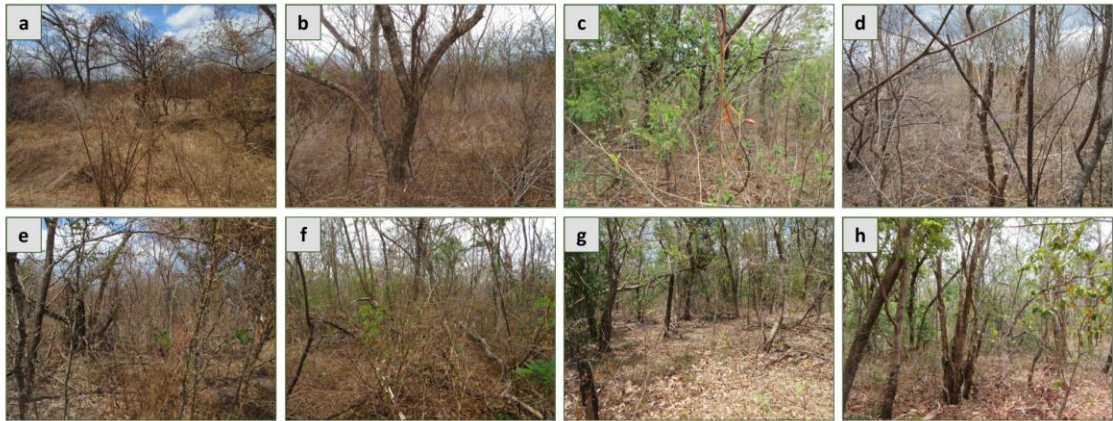


figure 24: photos of the edge and the forest interior of each transect in the dry season. a) T1 at 15m; b) T2 at 15m; c) T3 at 15m; d) T4 at 15m; e) T1 at 100m, f) T2 at 100m, g) T3 at 100m, h) T4 at 100m

When comparing the two measuring locations in the clear-cut note that the northern measuring location was only slightly more than 25m away from the forest in the north-western end of the clear-cut and was therefore surrounded by forest at 3 sides, while the clear-cut continued for more than 1km to the south from the southern measuring location at the clear-cut (figure 5, figure 4). At the southern measuring location the clear-cut was smaller than at the northern though, so that the distance to the forest to the west and east was about 20m each while in the north there was a distance of approximately 35m to the West 25m to the East (figure 5, figure 4). The vegetation on the whole clear-cut consisted of grass with only a few single trees (figure 25).

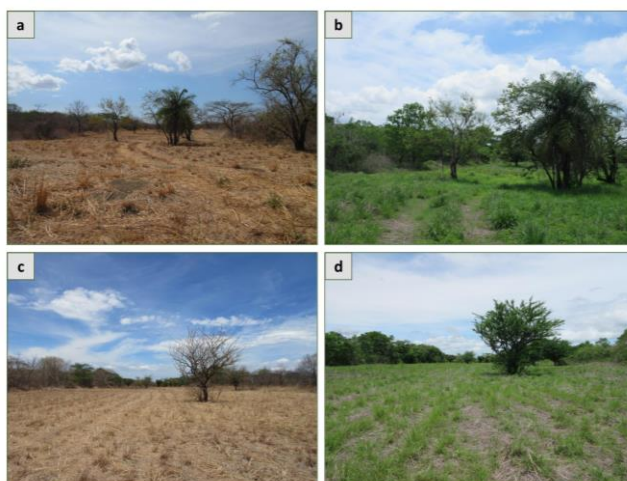


figure 25: photos of the clear-cut; a) southern measuring location facing north in the dry season; b) southern measuring location facing north in the rainy season; c) northern measuring location facing south in the dry season; d) northern measuring location facing south in the rainy season

For all measuring locations the amount of green vegetation increased clearly from dry to wet season (figure 24, figure 26). The temporal variation of canopy openness between the two seasons was highest for T4 with a difference of 27%, followed by T2 with a variation of 20%. T1 and T3 both had a difference of 10% between the canopy openness in the two seasons (table 8). With that, the spatial variance in canopy openness for the average values for all transects wasn't bigger between the seasons than between the different transects which was highest between T1 and T3 with a variance of 32% (table 8).



figure 26: photos of the edge and the forest interior of each transect in the rainy season. a) T1 at 15m; b) T2 at 15m; c) T3 at 15m; d) T4 at 15m; e) T1 at 100m, f) T2 at 100m, g) T3 at 100m, h) T4 at 100m

### 3.2 Comparison of temporal and spatial differences in CCMP

In the following the data of  $M_{\text{man}}$  will be examined. As the daily measurements were performed around the time of solar noon and thus closer to daily maximum temperatures than to minimum temperatures, lower temperatures in the data of  $M_{\text{man}}$  mean a higher buffering effect which is a higher CCMP.

Air and soil temperatures showed a high temporal variation and were lower in the wet season than in the dry season (figure 27, figure 28, Appendix B). Air temperatures in the dry season mostly varied from 32°C to 37°C while for the rainy season they mostly reached from 26°C to 34°C. A mean difference was thus around 4 and 5 K. For soil temperatures the range in the dry season generally was 30°C to 36°C and with 28°C to 30°C clearly lower for the rainy season with a mean difference of about 4 K. This confirms the first part of the hypothesis (I) which suggested that the CCMP is higher during the rainy season than during the dry season for the four transects.

Spatial variance of temperatures were generally not higher than temporal differences between the two seasons (figure 27, figure 28). During each day air temperatures usually varied about 1°C to 3°C between the different distances along the transect. For most of the days spatial differences of soil temperatures were also around 2°C. Soil temperatures partly reached higher temperature differences along the transect during a day of for example 5°C on 09.05.2018 in T1. Thus, generally the differences between the seasons were higher, than the spatial differences.

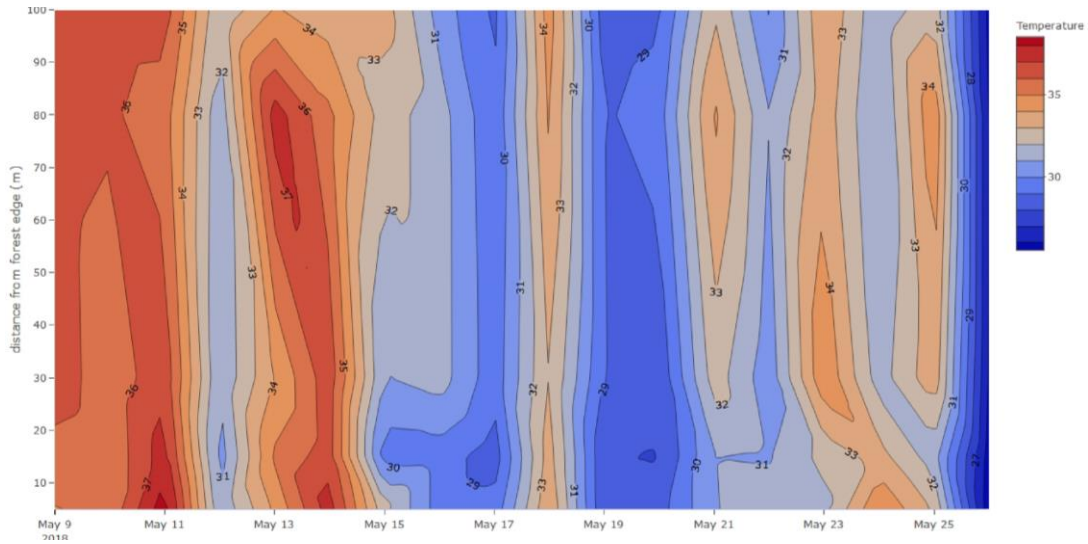


figure 27: time series of interpolated air temperatures with distance from forest edge in T1

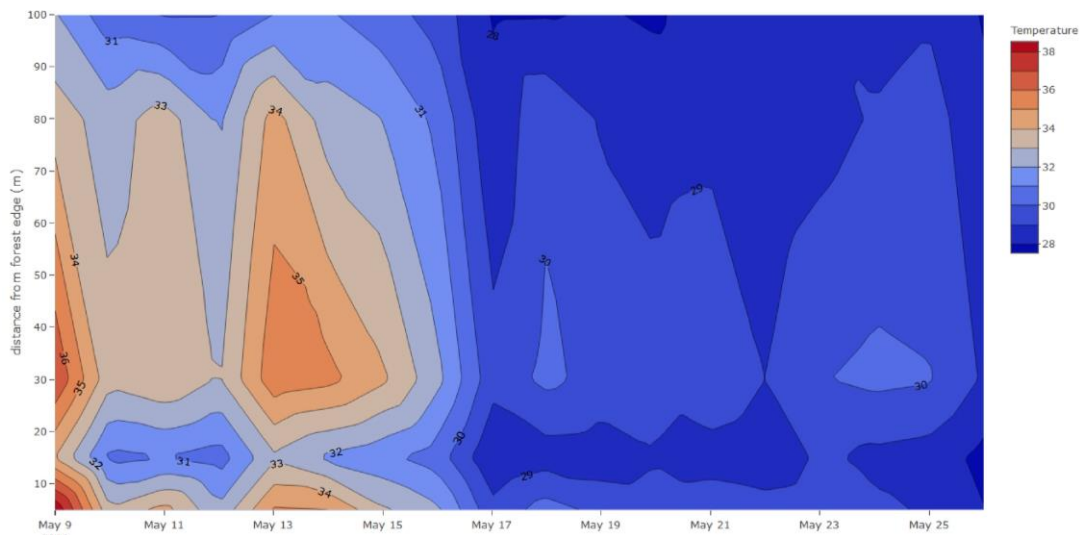


figure 28: time series of interpolated soil temperatures with distance from forest edge in T1

The temporal variation between the two seasons of the mean air and soil temperatures of the four transects were also higher than the spatial variance between the transects (figure 29). Mean air temperatures of the four transects had minima of approximately 31°C for the dry season and minima of 3°C less for the rainy season

except for the last day of the measuring period being even lower. The maxima in the dry season reached up to 37°C and only up to 3°C less for the rainy period. Mostly, the mean temperatures of the four transects only had a difference to each other of about 1°C to 2°C. The mean soil temperatures for each transect also had high differences before and after 15.05.2018 (figure 29). For the dry season the values were approximately between 30°C and 34°C whereas for the rainy season the soil temperatures varied from 28°C to 30°C except for the last day where temperatures reduced.

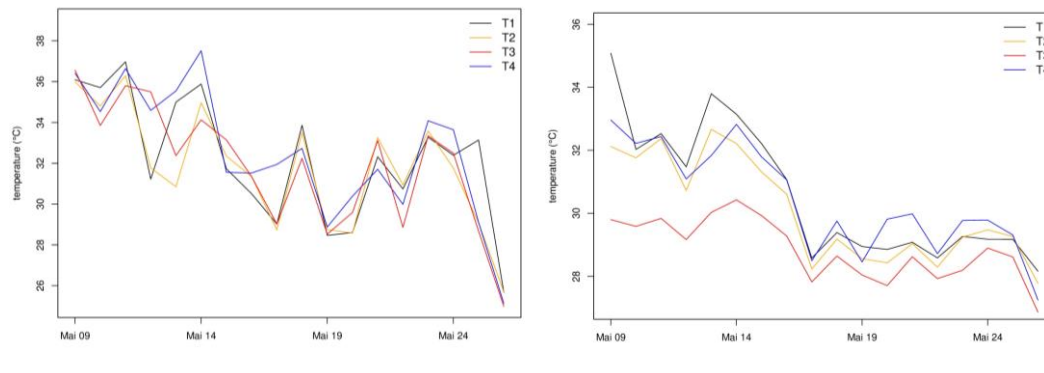


figure 29: mean air and soil temperatures of all five measuring locations for each transect

As shown in this analysis the data of  $M_{\text{man}}$  for the temperatures around solar noon suggests that the CCMP during the rainy season was higher than during the dry season and that the temporal differences in CCMP between the two seasons was higher than the spatial difference between the measuring points. This also applied to the automated data in T3. As the data of  $M_{\text{aut}}$  was collected during the whole day, the forest's buffering capability on temperatures was based on the temperature amplitude. A smaller temperature amplitude means a higher CCMP.

The distributions of the probability of the temperatures at the six measuring locations were similar (figure 30). When dividing the data into the measuring period before 15.05.2018 and the period afterwards, the mean probability densities of the temperatures of the measuring locations had clearly distinguishable distributions (figure 17). In table 3 it was shown that the kurtosis of the distribution of temperatures had a value lower than three for the dry season which indicates a platykurtic distribution. The distribution was thus flatter than the normal distribution which means that temperature extrema were reached more often. For the rainy season the value of the kurtosis was above three and the distribution therefore leptokurtic and thus showing the opposite deviation from the normal distribution. This indicates, that temperature extremes were

reached less often. Thus, CCMP was lower for the dry season than for the rainy season. The temporal differences of the temperature probability distributions were similar at all measuring locations (figure 31). With that the findings of the evaluation of  $M_{man}$  regarding temporal and spatial differences in CCMP could be confirmed with the data of the  $M_{aut}$ .

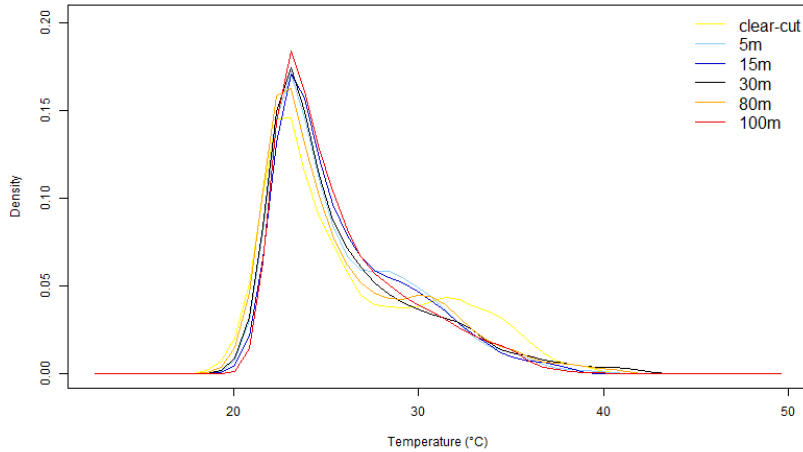


figure 30: probability density of temperatures in T3 for the whole period for all measuring locations; legend entries refer to horizontal distance from transect start

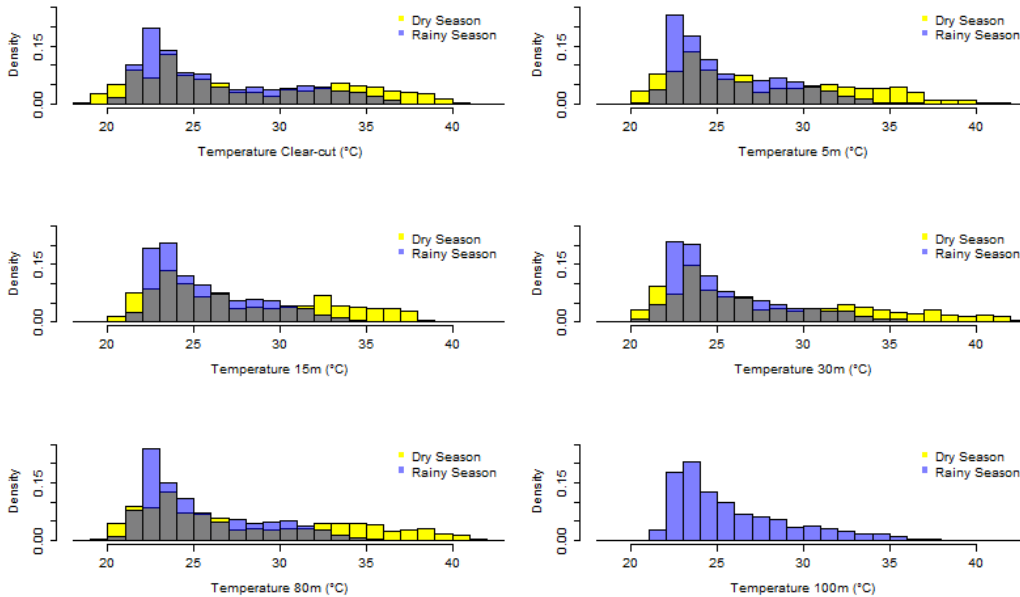


figure 31: probability density of temperatures in T3 for all measuring locations divided in dry and rainy season

Contrary to the first part of hypothesis (I), the second part which suggested that spatial differences compared to temporal differences would show higher disparities in CCMP was disproved. A plausible explanation is that while the density of vegetation

differed more between the transects and measuring locations within the transects than between the seasons, the amount of green leaves in the vegetation probably had higher seasonal than spatial differences. This could have a higher impact on the rate of evapotranspiration and with that on the buffer effect of temperatures than the vegetation density itself. Another important factor influencing the change of temperatures between the two seasons is the change of the precipitation rates and an increased humidity in all parts of the forest which additionally led to a cooling effect. As shown in the probability density distributions of absolute humidity in figure 32, the difference of humidity also showed a higher difference between the seasons than between the measuring locations along T3 from the clear-cut into the forest. This could explain why the temporal temperature difference are higher than the spatial differences. Another observation is that there are high daily differences in air temperatures of e.g. about 5K from 17.05.2018 to 18.05.2018. This could be due to a high influence of the current weather conditions such as wind and cloudiness on temperatures. The weather conditions in the last two days of the measurements with more constant rain in comparison to the rest of the measuring period, also affected the data by decreasing the temperatures. The generally higher amount of cloudy days in the rainy season than in the dry season could thus explain the high seasonal differences.

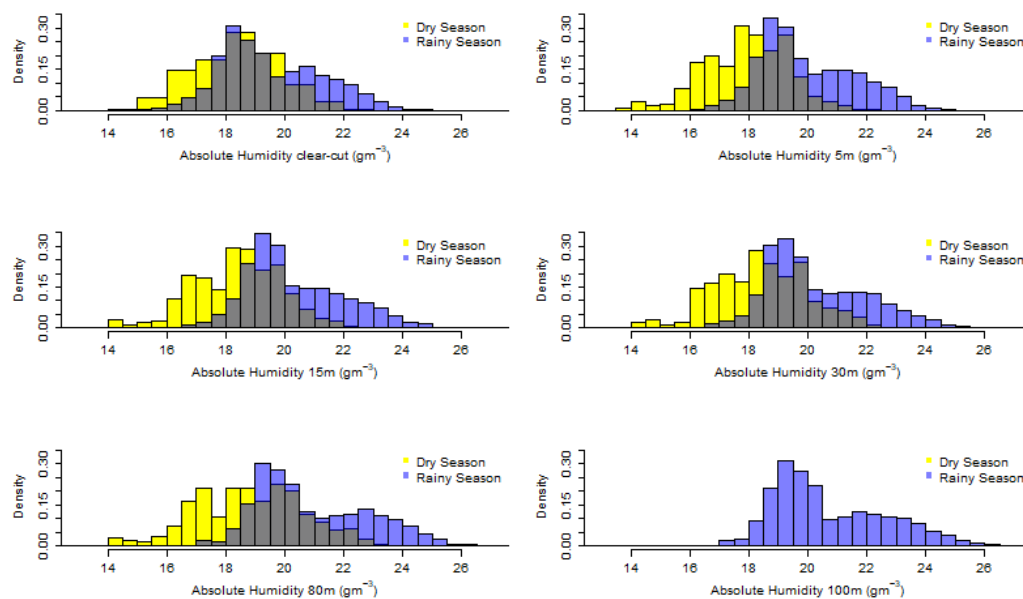


figure 32: probability density distribution of absolute humidity at all measuring locations in T3 divided in dry and rainy season

### 3.3 Comparison of the four transects regarding CCMP

In the following with the data of the  $M_{\text{man}}$  of mean air and soil temperatures of all measuring locations in the four transects hypothesis (II) will be evaluated. For the air temperatures the mean temperatures of the four transects were very close to each other and in the time series in figure 29 it can be seen, that for different days the order of the transects in regard of highest and lowest temperatures changed. The values of the temperatures for all four transects also fluctuated between the days in a range of more than four degrees (figure 29). For the mean air temperatures over the period of the dry and the rainy season respectively, the difference between the four transects was below two degrees for the dry season and below half a degree for the rainy season (figure 33, table 15).

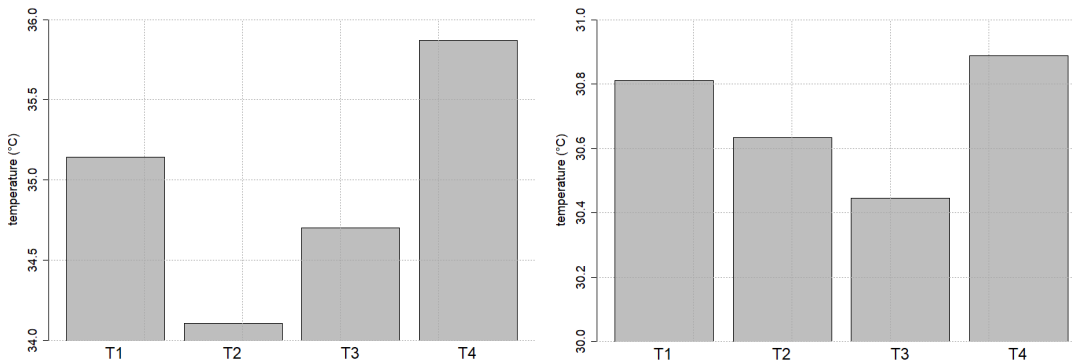


figure 33: mean air temperatures in dry and rainy season of all four transects

For the soil temperatures the order of the transects in regard of temperatures didn't change as much during the time and their differences to each other were higher than for the air temperatures especially during the dry season (figure 29). The change of the temperatures for each transect from day to day was mostly below 2K and therefore also lower than for the air temperatures. The difference of the mean soil temperatures of all transects was above 3 degrees for the dry season and just above 1 degree for the rainy season (figure 34). T3 had the lowest temperatures during the whole period and had a higher difference of temperatures to the other transect than those had to each other (figure 29). T2 had the second lowest temperatures for most of the days. The other two transects changed between generally having the highest and the second highest temperatures between the two seasons (figure 29).

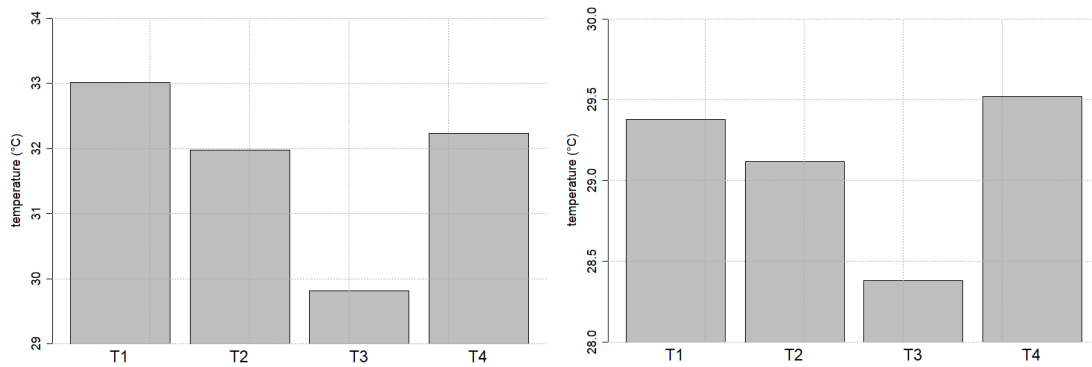


figure 34: mean soil temperatures in dry and rainy season of all four transects

The soil temperatures showed more stationary conditions than air temperatures. This can be explained by the soil having a higher heat capacity than the air (Ewers and Banks-Leite 2013). Additionally, the air temperatures are strongly influenced by turbulent transport processes.

During the rainy season for both, air and soil temperatures, the order of the four transects from lowest to highest was  $T3 < T2 < T1 < T4$  with T4 and T1 being very close to each other with a difference of  $0.1^{\circ}\text{C}$ . In the dry season in comparison to these results the air temperatures of T2 and T3 were reversed and the soil temperatures of T4 and T1. As for the data of the  $M_{\text{man}}$  lower temperatures mean a higher CCMP, the mitigation potential from high to low corresponds with the order of temperatures from low to high. Considering hypothesis (II) and the evaluated vegetation densities of 3.1, the expected order of the transects from high to low CCMP is T3, T4, T2 and T1. This could only partly be confirmed by measurements. For the first three transects, with the CCMP of  $T3 > T2 > T1$ , except for the air temperatures during the dry season, the hypothesis was verified. T4 on the other hand has the lowest CCMP instead of the expected second highest except for the soil temperatures in the dry season. A possible reason for the deviations of the hypothesis could be, that the vegetation analysis concentrated on density only. Leaf area, species composition, and forest structural properties can also be a reason for obtaining different temperature ranges for the understories at different sites (Portillo-Quintero et al. op. 2014). Differences in the colour of the vegetation could have led to a higher absorption of shortwave radiation due to a lower albedo in T4. As this would have led to a warming effect, CCMP of T4 would have been reduced. Additionally, the vegetation in T4 could have had a lower

transpiration rate and with that only a low cooling effect in comparison to the other transects. This would explain temperatures in T4 being higher and with that CCMP of T4 being lower than for the other transects. Furthermore, for this analysis trees with a diameter above 10cm and lianas with a diameter above 5cm were considered, excluding all sorts of shrubs, herbs and smaller trees. A high density of shrubs in the understory of T4 could have reduced turbulent air exchange, causing a decrease of evapotranspiration. This is because relative humidity in the air directly above the surfaces at which evapotranspiration occurs, increases due to the vaporization. With increased relative humidity of the air further evapotranspiration rates are reduced. For low wind speeds, there is a low mixing of the air. Consequently, the air close to water or leaf surfaces with higher humidity isn't transported away from these surfaces as effectively as for high wind speeds so that evapotranspiration rates decrease. So, the forest's cooling effect during the day and thus CCMP could have decreased.

### **3.4 Comparison of gradients of CCMP within the four transects**

Figure 35 and figure 36 show the air and soil temperatures in the four transects divided in the parts clear-cut, edge and forest interior for both seasons. Also displayed is the standard deviation between the three measuring locations in the edge and the two measuring locations in the forest interior for each transect. In the following the gradient of air and soil temperatures along the transects from clear-cut to forest interior will be examined to test hypothesis (III).

Air temperatures generally increased from the clear-cut over the edge to the forest in the four transects with two exceptions: for T1 there was a small decrease of less than 0.1 degrees from the edge to the forest, which is within the area of the standard deviation and for T3 there was a temperature increase from edge to forest, but the value of the clear-cut was higher (Figure 35). This is also within the area of the standard deviation of the forest interior. In the rainy season for T1 there was still an increase of air temperatures from clear-cut to forest interior (Figure 35). For T2 to T4 temperatures increased from the edge to the forest interior, but in T2 the clear-cut had a lower temperature. For T4 the clear-cut's temperature was between the temperatures of the clear-cut and the forest, but within the standard deviation of both, edge and forest. Only for T3 there was a decrease from clear-cut to edge to forest interior (Figure 35). The

temperatures of the edge and interior were very close to each other with a difference below 0.1 degree and a standard deviation of about half a degree (Figure 35).

Generally, the differences between the mean air temperatures of clear-cut, edge and forest decreased from dry to rainy season, meaning that the temperature amplitude along a transect was higher during the dry season than during the rainy season. For T4 e.g. the gradient from clear-cut to forest interior was 1°C during the dry season and only about 0.25°C in the rainy season (Figure 35). There was one exception of T3 where the amplitude is 0.5°C for both seasons (Figure 35).

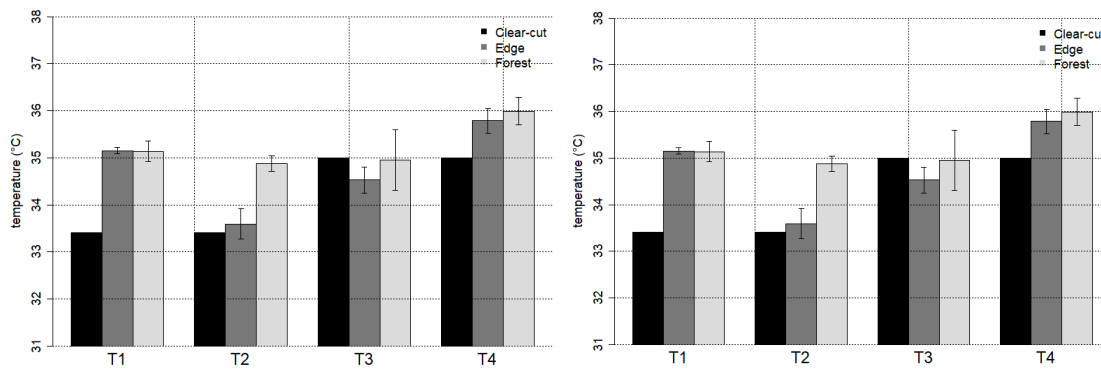


Figure 35: mean air temperatures divided in clear-cut, edge and forest interior in dry season and rainy season

The gradients of the soil temperature for the dry season decreased from clear-cut to forest for T1 and T2 (figure 36). For T3 the temperature from clear-cut to the edge also decreased, but there was an increase from the edge to the forest. For T4 the temperatures decreased from edge to forest like in T1 and T2, but the mean temperature of the clear-cut was in between the temperatures of the edge and the forest in T4. In the rainy season the temperature gradients resembled those in the dry season, but the temperature differences within the transects were smaller. For T4 the temperature of the edge was still the highest, while the forest had a similar value as the clear-cut (figure 36).

Like for the air temperatures, the amplitude of the soil temperatures was smaller in the rainy season than in the dry season (figure 36). The differences of the amplitudes between the seasons were higher for soil temperatures than for air temperatures. The amplitude in T3 for example reduced from about 2°C to less than 1°C (figure 36).

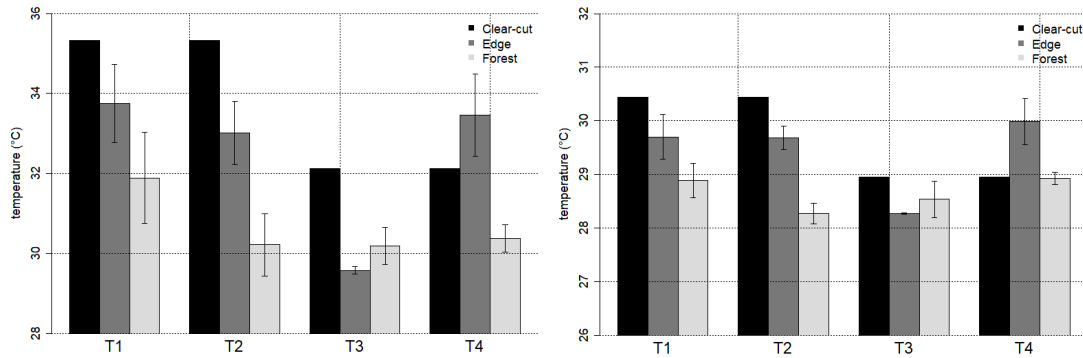


figure 36: mean soil temperatures divided in clear-cut, edge and forest interior in dry season and rainy season

With the first part of hypothesis (III), an increase of CCMP from clear-cut over edge to forest interior for both seasons was hypothesized. Different results were obtained when looking at soil and air temperatures. For the air temperatures in the dry season the hypothesis couldn't be confirmed. Instead for T1, T2 and T4 the gradient was mostly reversed with a high CCMP at the clear-cut and a decrease over the edge to the forest. A possible reason is a darker colour of the forest in comparison to the clear-cut, as the forest's vegetation was mostly woody and as the leaves on the trees were mature in the end of the dry season and with that of a darker green. Thus, albedo was lower inside the forest so that a warming effect due to the absorption of shortwave radiation was higher. Furthermore, a small amount of green vegetation that transpired in the transects during the dry season likely caused only a small cooling effect by evapotranspiration. Additionally, the vegetation probably decreased the wind speed inside the transects especially in the forest interior and partially at the forest edge, which diminished air exchange and with that rates of evapotranspiration. In Davies-Colley et al. (2000) wind strength inside the transects in the forest was clearly lower than at the open land reaching only an average of wind exposure of 20% inside the forest compared to the open land. A similar effect in the tropical dry forest is probable.

In T3 on the other hand temperatures in the transect were lower than at the clear-cut, partly supporting the first part of hypothesis (III). Contrary to the hypothesis, the mean temperature in the forest interior was higher than in the edge though. This transect had the densest vegetation and had more green vegetation which transpired during the dry season than the other three transects. The mature green leaves had a darker colour than the woodier vegetation in the other transects. Due to the albedo differences T3 had a

higher warming effect than the other transects, but this seems to be outweighed by the higher cooling effect due to evaporation.

For the rainy season for T1 the CCMP inside the transect is lower than at the clear-cut. As this transect had the sparsest vegetation, the rates of evaporation might still have been low during the rainy season. For the other three transects the CCMP decreased from edge to forest, partly supporting the first part of hypothesis (III), but the clear-cut's CCMP in comparison to the edge and the forest was different for each transect. The different temperatures at the clear-cut, could be due to differences in wind speed with higher wind speeds increasing evaporation rates and thus having a cooling effect. The northern measuring location at the clear-cut was close to the forest edge in the north which can have decreased wind speeds, while the southern measuring location was further away from the northern and the southern forest edges. Thus, higher wind speeds at the southern location are plausible. Overall, for the air temperatures the first part of hypothesis (III) couldn't be verified.

The order of the CCMP on the base of the soil temperatures for T1 and T2 matched up with the first part of hypothesis (III) in both seasons, while in T3 the edge's and forest's CCMP are exchanged and for T4 the clear-cut's CCMP is higher in comparison with the edge and the forest than expected during both seasons. In Davies-Colley et al. (2000) study soil temperatures insight the transect decreased corresponding with the increase of shade while for air temperatures a decrease inside the forest wasn't detected directly with the decrease of sunlight exposure. Accordingly, the reason for the soil temperatures showing a different order during the dry season than the air temperatures could be due to an additional cooling effect of shadow by the vegetation which might have had a greater influence on the soil than on the air temperatures. Thus, for the soil temperatures the first part of hypothesis (III) mostly applies.

For both, air and soil temperatures, it was shown that the differences in CCMP within the transects were higher during the dry than during the rainy season which isn't consistent with the second part of hypothesis (III). This could be related to the fact that during the dry seasons the conditions were mostly sunny while during the rainy season the sky was mostly overcast. A previous study showed high gradients from open land to the forest interior for sunny days while on overcast days these gradients were very small (Davies-Colley et al. 2000). This could be the reason why a higher gradient of

temperatures along the transects was obtained in the dry season than during the rainy season.

The temperatures of T3 will be analysed more in detail in the following part which refers to the data of the  $M_{\text{aut}}$ . The median value of the temperatures was lowest for the edge in both seasons and during the dry season second lowest for the clear-cut and highest for the forest, while it was second lowest for the forest and highest for the clear-cut in the rainy season (figure 37). Higher values of the median for the forest interior and for the clear-cut than for the forest edge are consistent with the findings of Portillo-Quintero et al. (op. 2014) where the temperature values decreased at 4 to 16m from the forest edge and from there increased with distance from the edge. The minima temperatures increased from clear-cut over edge to the forest interior in both seasons. The lowest maxima temperatures were reached at the clear-cut for both seasons while there was a difference of the order between edge and forest interior the two seasons: in the dry season the lower maxima temperatures were reached by the forest and the edge had the highest temperatures and in the rainy season it was reversed. With that, the gradients between clear-cut, edge and forest in regard of maxima temperatures were consistent with the measurements of the  $M_{\text{man}}$ . The highest amplitude of minima and maxima temperatures was  $23.3^{\circ}\text{C}$  and was measured at the edge during the dry season. The clear-cut and forest interior followed with similar amplitudes of 21.8 degrees and 21.6 degrees respectively. In the rainy season it was highest for the forest and lowest for the clear-cut with the edge being in the middle. The gradient of temperature amplitudes within the transects was by 1.2 degrees higher during the dry season than during the rainy season.

The temperature distributions showed different shapes especially for the maxima temperatures. For the edge during both seasons and for the forest interior during the rainy season the distributions are very thin for high temperatures, indicating that there were only single values which might be outliers of maxima temperatures. Due to these differences in the distributions, the quantification of CCMP won't be based on the temperature amplitude, but the IQR will be considered. The IQR had the lowest value for the edge during the dry season, while the other two areas were with 0.1 degrees difference very close to each other. In the rainy season, both the edge and the forest had lower values than the clear-cut and were with 4.7 degrees (edge) and 4.9 degrees (forest interior) close to each other. The range of the IQR between the areas increased from dry to rainy season by 0.5 degrees.

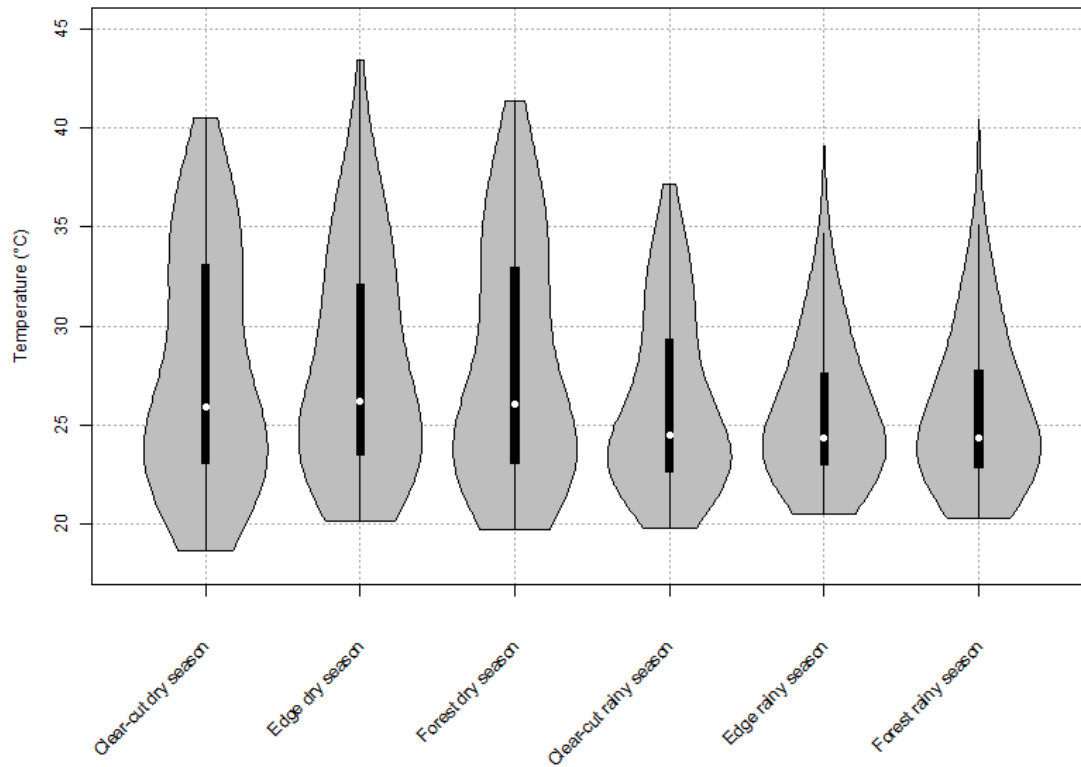


figure 37: Violin plots of air temperatures in the areas clear-cut, edge and forest interior in T3 for dry and rainy season

Based on the IQR, during both seasons the CCMP was highest for the edge and second highest for the forest interior followed by the clear-cut.

Hypothesis (III) stated that the forest would have the highest CCMP followed by the edge and the clear-cut. The clear-cut having the lowest CCMP could be verified in T3, but the order of edge and forest was exchanged for both seasons. Portillo-Quintero et al. (op. 2014) found slightly lower temperatures in up to 20m from the forest edge. The authors explain this with the vegetation composition in the exposed conditions at the edge where rapid-growth trees, shrubs and lianas are abundant and change the microclimatic conditions in comparison to the forest interior. This could also be the reason for the CCMP being higher in the forest edge in T3 than in the interior. Another explanation could be the vegetation being denser at the measuring location at 30m than at 80m and 100m causing a stronger cooling effect at the edge than in the interior.

The second part of hypothesis (III) could be verified when looking at the amplitudes and IQR in T3 instead of the maxima temperatures. The differences between the temperature amplitudes and the IQRs within the transects were smaller during the dry season than during the rainy season (figure 8, table 16).

#### 4 Conclusion

The results showed that CCMP differences of the whole transects were higher between the two seasons than between the transects, suggesting that seasonality has a higher impact than vegetation differences in the tropical dry forest. The comparison of CCMP between the four transects showed for three transects that higher vegetation density also means a higher CCMP of the forest. The analysis of the temperature gradients along the transects showed that the forest interior didn't generally have a higher mitigation potential than the clear-cut for transects with lower vegetation density. The transect with the densest vegetation on the other hand had a higher CCMP at the edge and in the forest interior than at the clear-cut.

Considering this, a high vegetation density is decisive for CCMP of tropical dry forests. Generally, older forests have a higher vegetation density as the vegetation had more time to grow. For climate change mitigation it is thus worthwhile to protect existing tropical dry forests in later successional states. If reforestation efforts are made, it is of importance that the protection of the reforested area is ensured on long-term. In the first years, when the forest's vegetation is still sparse CCMP is low. With the growing of the forest over the years, CCMP increases. The forest in the study area, which was in an intermediate succession and 15 to 30 years old partly showed higher and partly lower CCMPs in the forest than at a clear-cut. From the study in this area it can be assumed that TDFs which are older than 15 to 30 years increase climate change mitigation while younger forests might have a decreasing effect on CCMP. Other components than age, such as regionally varying environmental factors like soils and climate should also be considered for forest growth. Besides that, there are further aspects than a buffering effect on temperatures which are relevant for climate change mitigation. So, e.g. carbon sequestration by tropical dry forest also needs to be considered when discussing the forest's climate change mitigation potential. Other environmental benefits such as the protection of biodiversity are an additional reason for protecting tropical dry forests.



## **Acknowledgements**

My thanks go to everyone who supported me during the work on this thesis.

Especially, I want to thank my supervisor Prof. Dr. Christoph Thomas for making this project possible, providing me with many new ideas and enthusiastically supporting me during the whole process of making this thesis.

Special thanks also go to Prof. Dr. Arturo Sánchez-Azofeifa for providing the opportunity of carrying out our measurements at Santa Rosa National Park, for the support regarding the decision of the measurement set-up, and for giving an introduction to the ecosystem's characteristics and to methods of data collection during a summer school.

Furthermore, I want to thank my second supervisor Dr. Wolfgang Babel and the whole micrometeorology group for the support during this work.

Thank you to Sofia for the support at Santa Rosa National Park during our measurements and for helping us out with our lack of Spanish skills.

And, of course, special thanks go to Elena and Anna for the great team work and for the adventurous time in Costa Rica full of new experiences. Additional thanks to Elena, for the help with R.

Besides the above-mentioned I would like to thank my family and my boyfriend for the great support during the whole bachelor programme.



**Appendix A: Specification measurement devices**

table 9: short-term manual measurements

<b>sensor</b>	<b>Measured parameter</b>	<b>unity</b>	<b>Height from surface (m)</b>
integrated in device: “testo 480 – Klimamessgerät”	air pressure	hPa	1
temperature sensor: “Wasserdichter Tauch-/Einstechfühler (TE Typ K)”(Testo)	Soil temperature	°C	0.077 (into the soil)
temperature sensor: PT100 “Lufttemperatur-Fühler Pt100”(Testo)	Air temperature	°C	1
hot wire probe: “Hitzdraht Sonde (Ø 10 mm) - für Strömung, Temperatur, Feuchte, Druck”(Testo)	wind speed	ms <sup>-1</sup>	2
	air temperature	°C	
	relative humidity	%	

table 10: contineous automated measurements

<b>sensor</b>	<b>Measured parameter</b>	<b>unity</b>	<b>Heigth from surface (m)</b>
Funky_Clima “kapazität-Halbleitersensor”(Cosmos data AG 2005)	Air temperature	°C	1
	Relative humiditiy	%	

table 11: weather station

<b>device</b>	<b>Measured parameter</b>	<b>unity</b>	<b>Heigth from surface (m)</b>
Weather station Ma4100	Solar Radiation	$\text{Wm}^{-2}$	1
	Precipitation	mm	
	Lightning Activity	-	
	Lightning Distance	km	
	Wind Direction	$^{\circ}$	
	Wind Speed	$\text{ms}^{-1}$	
	Gust Speed	$\text{ms}^{-1}$	
	Air Temperature	$^{\circ}\text{C}$	
	Relative Humidity	%	
	Atmospheric Pressure	kPa	
	Maximum Precipitation Rate	$\text{mmh}^{-1}$	

table 12: Wireless Sensor Network Station 1

<b>device</b>	<b>Measured parameter</b>	<b>unity</b>	<b>Heigth from surface (m)</b>
Wireless Sensor Network	Air temperature	$^{\circ}\text{C}$	1
	atmospheric pressure	hPa	
	relative humidity	%	
	radiation	$\text{Wm}^{-2}$	
	soil moisture	%	

**Appendix B: Additional figures**

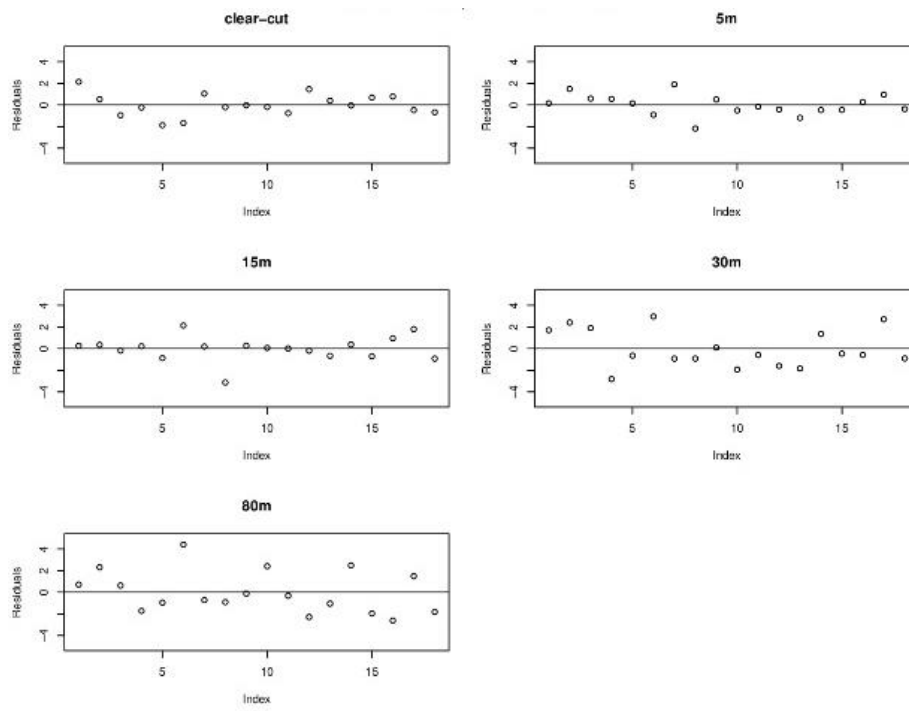


figure 38: residuals of comparison of  $M_{aut}$  and  $M_{man}$  in temperatures ( $^{\circ}C$ )

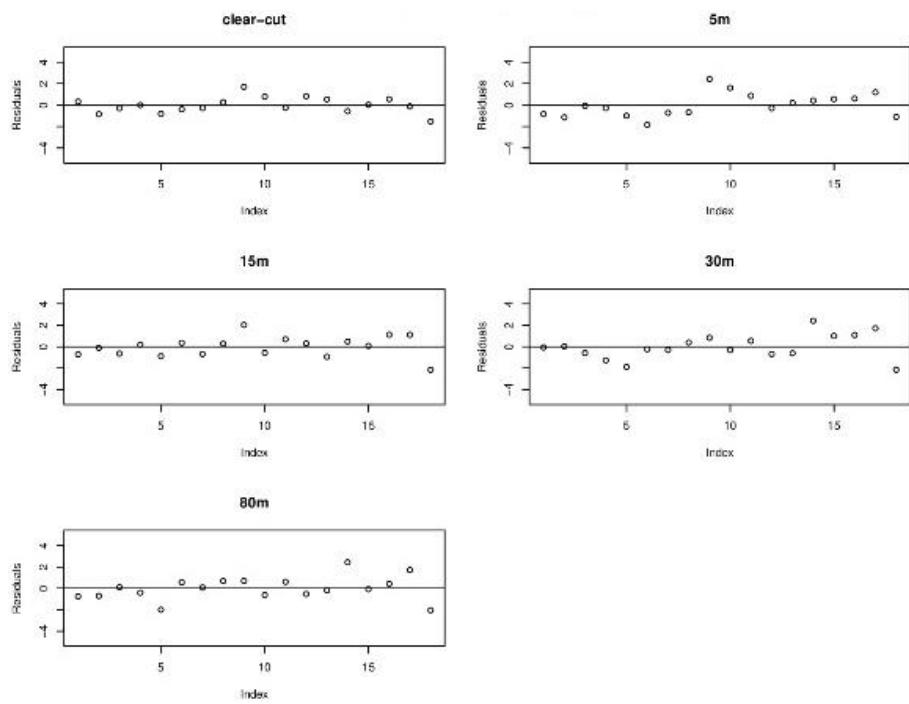


figure 39: residuals of comparison of  $M_{aut}$  and  $M_{man}$  in humidity ( $gm^{-3}$ )

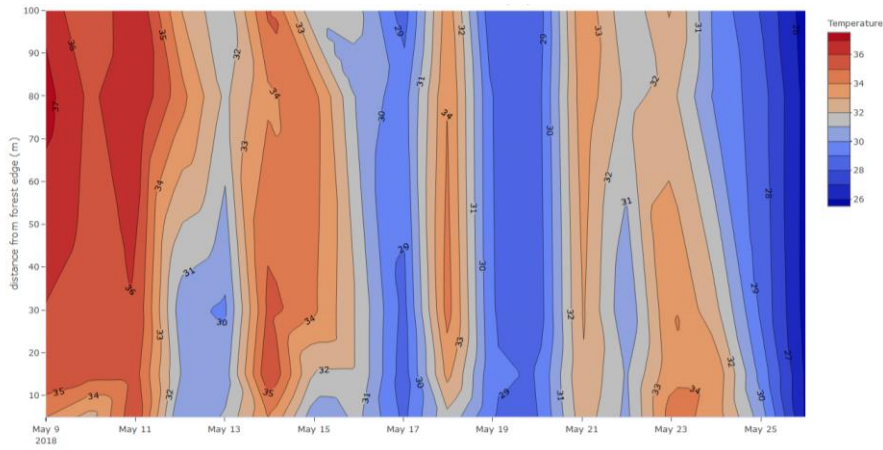


figure 40: time series of interpolated air temperature in T2

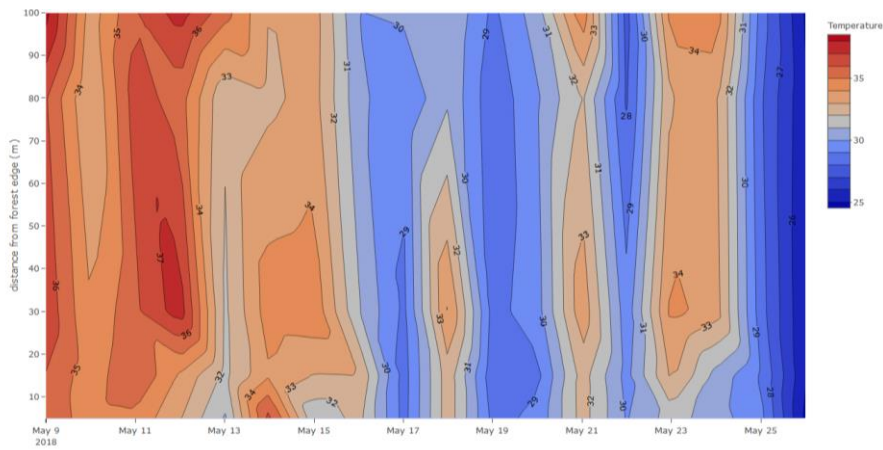


figure 41: time series of interpolated air temperature in T3

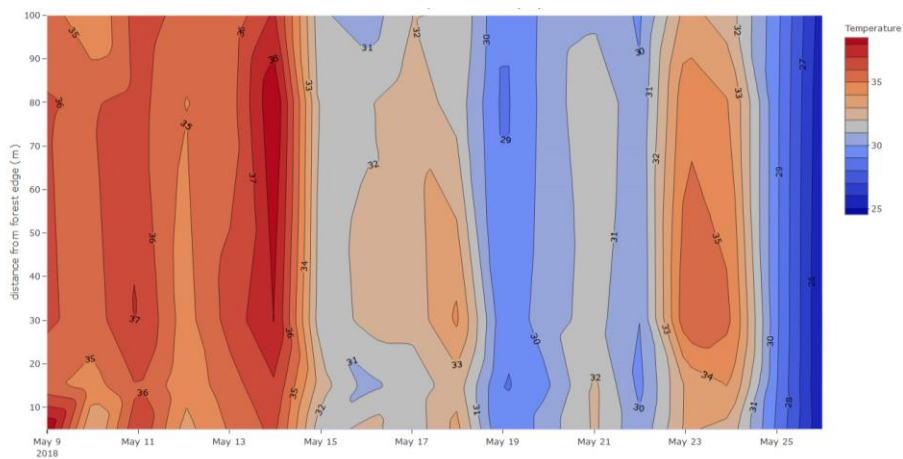


figure 42: time series of interpolated air temperature in T4

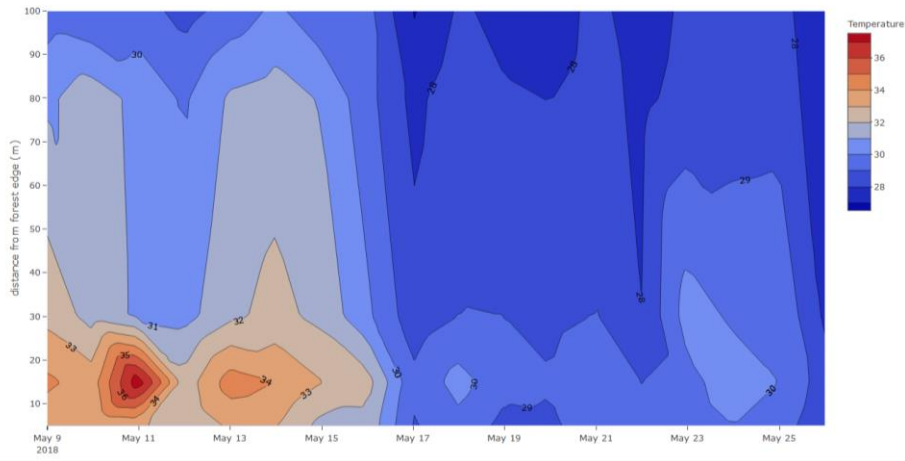


figure 43: time series of interpolated soil temperature in T2

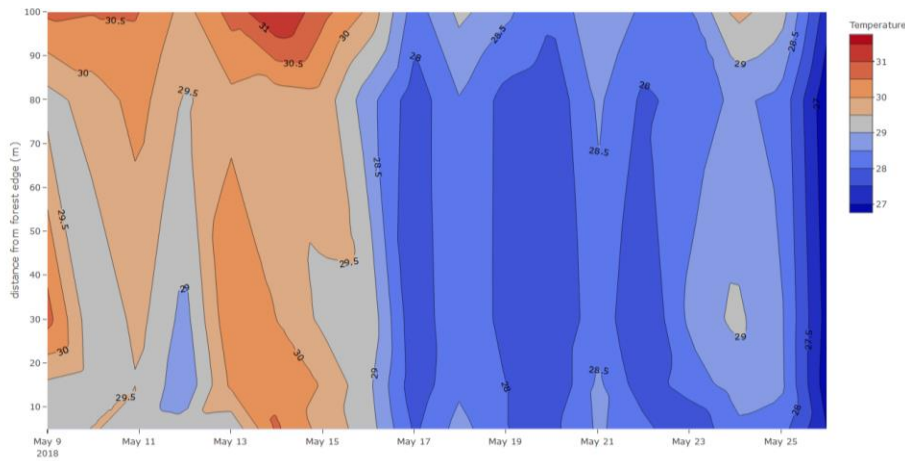


figure 44: time series of interpolated soil temperature in T3

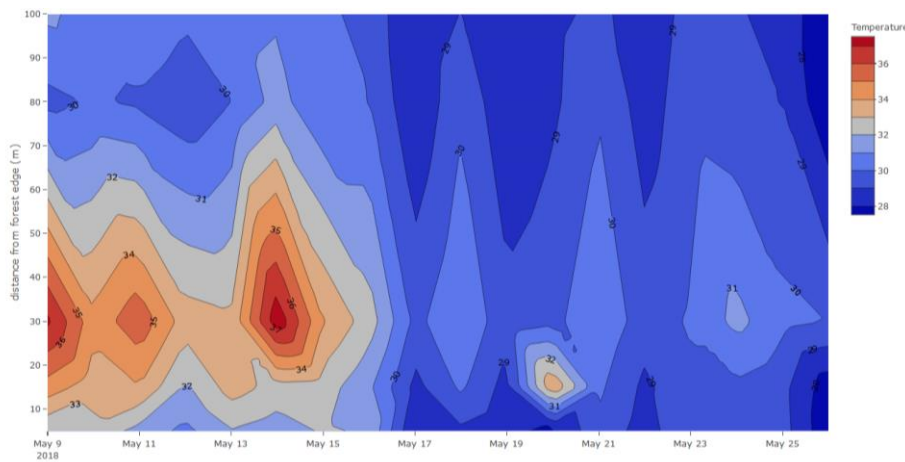


figure 45: time series of interpolated soil temperature in T4



**Appendix C: Additional photos**

table 13: photos of the measuring locations at 5m, 30m and 80m from transect start for all transects in the dry season

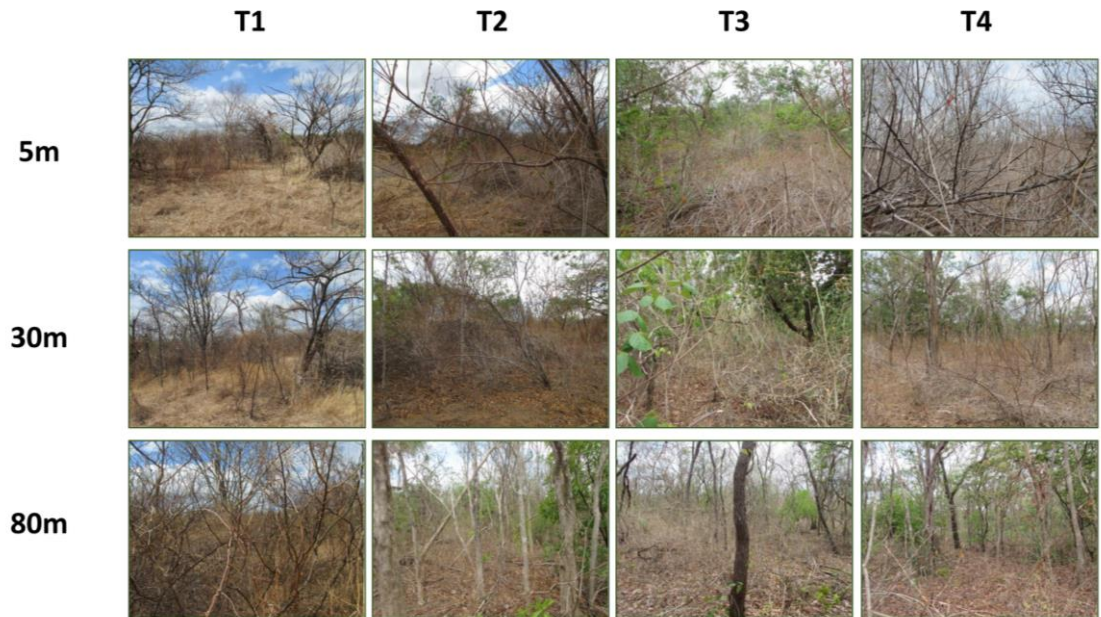
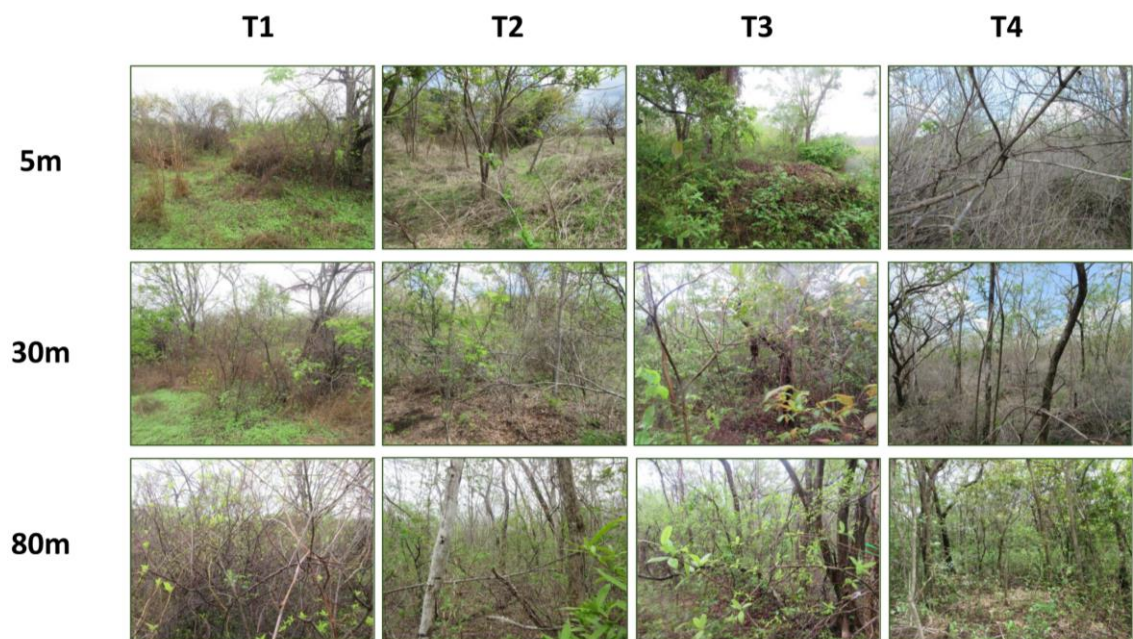


table 14: photos of the measuring locations at 5m, 30m and 80m from transect start for all transects in the rainy season





**Appendix D: Additional tables**

table 15: mean air and soil temperatures in dry and rainy season of all four transects

	T1	T2	T3	T4
air dry season	35.1°C	34.1°C	34.7°C	35.9°C
air rainy season	30.8°C	30.6°C	30.4°C	30.9°C
soil dry season	33.0°C	32.0°C	29.8°C	32.2°C
soil rainy season	29.4°C	29.1°C	28.4°C	29.5°C

table 16: temperature amplitude and interquartile range of temperatures in the different areas in dry and rainy season:

	dry season			rainy season		
	clear-cut	edge	forest	clear-cut	edge	forest
amplitude	21.8°C	23.3°C	21.6°C	17.3°C	18.5°C	20.2°C
IQR	10.0°C	8.6°C	9.9°C	6.6°C	4.7°C	4.9°C



## Bibliography

- Akima, Hiroshi (1974): Bivariate interpolation and smooth surface fitting based on local procedures. In *Commun. ACM* 17 (1), pp. 26–31. DOI: 10.1145/360767.360797.
- Calvo-Alvarado, J.; McLennan, B.; Sánchez-Azofeifa, A.; Garvin, T. (2009): Deforestation and forest restoration in Guanacaste, Costa Rica: Putting conservation policies in context. In *Forest Ecology and Management* 258 (6), pp. 931–940. DOI: 10.1016/j.foreco.2008.10.035.
- Cao, S.; Sanchez-Azofeifa, G. A.; Duran, S. M.; Calvo-Rodriguez, S. (2016): Estimation of aboveground net primary productivity in secondary tropical dry forests using the Carnegie–Ames–Stanford approach (CASA) model. In *Environ. Res. Lett.* 11 (7), p. 75004. DOI: 10.1088/1748-9326/11/7/075004.
- Cosmos data AG (Ed.) (2005): Miniaturmesslogger. funky-Clima Version 1.01. Benutzerhinweise.
- Davies-Colley, R.; van Payne, G. W.; van Elswijk, M. (2000): Microclimate gradients across a forest edge. In *New Zealand Journal of Ecology*. 24.
- Diffenbaugh, Noah S.; Singh, Deepti; Mankin, Justin S.; Horton, Daniel E.; Swain, Daniel L.; Touma, Danielle et al. (2017): Quantifying the influence of global warming on unprecedented extreme climate events. In *Proceedings of the National Academy of Sciences of the United States of America* 114 (19), pp. 4881–4886. DOI: 10.1073/pnas.1618082114.
- Ewers, Robert M.; Banks-Leite, Cristina (2013): Fragmentation Impairs the Microclimate Buffering Effect of Tropical Forests. In *PLoS ONE* 8 (3). DOI: 10.1371/journal.pone.0058093.
- Foken, Thomas (2016): Angewandte Meteorologie. Mikrometeorologische Methoden. 3. Auflage. Berlin, Heidelberg: Springer Spektrum. Available online at <http://dx.doi.org/10.1007/978-3-642-25525-0>.
- Friedl, M. A. (2002): Forward and inverse modeling of land surface energy balance using surface temperature measurements. In *Remote Sensing of Environment* 79 (2-3), pp. 344–354. DOI: 10.1016/S0034-4257(01)00284-X.

Hoekstra, Jonathan M.; Boucher, Timothy M.; Ricketts, Taylor H.; Roberts, Carter (2005): Confronting a biome crisis: global disparities of habitat loss and protection. In *Ecology Letters* 8 (1), pp. 23–29. DOI: 10.1111/j.1461-0248.2004.00686.x.

Li, Yan; Zhao, Maosheng; Motesharrei, Safa; Mu, Qiaozhen; Kalnay, Eugenia; Li, Shuangcheng (2015): Local cooling and warming effects of forests based on satellite observations. In *Nature communications* 6, p. 6603. DOI: 10.1038/ncomms7603.

Portillo-Quintero, Carlos; Sánchez-Azofeifa, Arturo; Marcos do Espírito-Santo, Mário (op. 2014): Edge Influence on Canopy Openness and Understory Microclimate in Two Neotropical Dry Forest Fragments. In Gerardo-Arturo Sánchez-Azofeifa, María de Jesús Aguilar-Aguilar (Eds.): *Tropical dry forests in the Americas. Ecology, conservation, and management*. Boca Raton: CRC Press Taylors & Francis Group, pp. 157–172.

R Core Team (2018): R: A language and environment for statistical computing. . . Vienna, Austria: R Foundation for Statistical Computing. Available online at <https://www.R-project.org/>.

Raper, Sarah C. B.; Braithwaite, Roger J. (2006): Low sea level rise projections from mountain glaciers and icecaps under global warming. In *Nature* 439 (7074), pp. 311–313. DOI: 10.1038/nature04448.

Sánchez-Azofeifa, A.; Kalacska, M.; Quesada, M.; Calvo-Alvarado, J.; Nassar, M.; Rodriguesz, J.; Paulo, N. (2005): Need for Integrated Research for a Sustainable Future in Tropical Dry Forests. In *Conservation Biology* 19 (2), pp. 285–286. DOI: 10.1111/j.1523-1739.2005.s01\_1.x.

Sánchez-Azofeifa, Gerardo Arturo; Guzmán-Quesada, J. Antonio; Vega-Araya, Mauricio; Campos-Vargas, Carlos; Durán, Sandra Milena; D'Amico et al. (2017): Can terrestrial laser scanners (TLSs) and hemispherical photographs predict tropical dry forest succession with liana abundance? In *Biogeosciences* 14 (4), pp. 977–988. DOI: 10.5194/bg-14-977-2017.

Testo (Ed.): Pt100 Fühler · hochpräzise Tauch-, Luft- und Einstechfühler. 0614 0073, 0614 0072, 0614 0275. Anwendungshinweis.

Testo (Ed.): Thermische Strömungsmesssonde. Anwendungshinweis.

Thomas, Christoph K.; Law, Beverly E.; Irvine, James; Martin, Jonathan G.; Pettijohn, J. Cory; Davis, Kent J. (2009): Seasonal hydrology explains interannual

and seasonal variation in carbon and water exchange in a semiarid mature ponderosa pine forest in central Oregon. In *J. Geophys. Res.* 114 (G4), p. 714. DOI: 10.1029/2009JG001010.

Zvomuya, Francis; Larney, Francis J.; McGinn, Sean M.; Olson, Andrew F.; Willms, Walter D. (2008): Surface Albedo and Soil Heat Flux Changes Following Drilling Mud Application to a Semiarid, Mixed-Grass Prairie. In *Soil Science Society of America Journal* 72 (5), p. 1217. DOI: 10.2136/sssaj2007.0430.



**Declaration of Authorship**

I herewith certify that the work presented above is to the best of my knowledge and belief original and the result of my own investigations. Third party work, non-published and published information I received are properly and duly acknowledged. This work has never previously been submitted to any other examination committee.

Bayreuth, 21.12.2018

---

(Marie Stöckhardt)